Material Matters™

ALDRICH®
Materials Science

Methods for Nanopatterning and Lithography

Patterning Tomorrow's Electronics

Hexafluoroalcohol-functionalized Methacrylate Monomers for Lithographic/Nanopatterning Materials

Inkjet Printing as a Key Enabling Technology for Printed Electronics

Conductive Polymers for Advanced Micro- and Nano-fabrication Processes

Micro and Nanometer Scale Photopatterning of Self-assembled Monolayers

SIGMA-ALDRICH®

Introduction

Welcome to the first 2011 issue of *Material Matters™* entitled *Methods for Nanopatterning and Lithography*. This issue describes a number of methods used to create patterned material features on the nanoscale, which are crucial in the generation of electronic devices. There are a variety of techniques for fabricating on sub-micron-length scales, spanning from sophisticated, top-down lithographic methods that have their origins in the electronics industry to more recent advancements incorporating bottom-up approaches that rely on self-organization. For nanopatterning, several approaches of both types have been proposed and well-demonstrated.

Kaushik Patel, Ph.D.
Materials Science
Sigma-Aldrich Corporation

The vast majority of electronic devices today are fabricated using top-down photolithographic techniques that rely on sophisticated, cutting-edge instrumentation and tailored materials. For example, a typical integrated circuit consists of various patterned thin films of metals, dielectrics and semiconductors on substrates including silicon, gallium arsenide, or germanium. Such a device is generally fabricated by lithography, where radiation-sensitive polymeric materials called resists are used to produce desired circuit patterns in the substrates. However, the search still continues for non-photolithographic methods, which could provide technologically simpler and more cost-effective nanofabrication strategies. Such methods, some of which are described in this issue, include nano-imprint lithography (including micro-contact printing, mold-assisted lithography, and hot embossing lithography), near-field optical lithography, direct patterning on the nanometer scale using scanning-probe microscopes or inkjet printing systems, self-assembly of monolayers, etc.

Some of these approaches are better suited for producing individual nano-structures for the investigation of nanometer-scale devices; the throughput is likely to remain impracticably low for commercial application. Others, such as nanoimprint lithography, have the potential of high throughput due to parallel processing, less sophisticated tools, and nanoscale replication for applications such as data storage. Some new developments, including a number of key enabling materials designed to relieve some of the high-resolution challenges, are presented in this issue.

The issue begins with an article by researchers at the IBM Almaden Research Center (San Jose, California) who utilize fluorinated methacrylate polymers as high-static, highly soluble photoresists for 193 nm lithography. In the following article, researchers at the Fraunhofer Institute and Chemnitz University of Technology, Germany, describe the versatility of inkjet printing technology in the direct-write fabrication of electronic structures on a variety of rigid and flexible substrates. Professor Rahman and his colleagues (University of Glasgow, UK) show the use of conductive polymers as charge dissipation layers for state-of-the-art high resolution patterning techniques, including electron-beam lithography. The final article by Professor Graham Leggett shows an elegant, combined bottom-up and top-down photochemical approach using alkylphosphonic acid monolayers. Patterns are created on the monolayer by either (i) applying a mask and subsequent exposure to UV light or (ii) coupling a scanning near-field optical microscope with a UV laser to obtain <10 nm resolution.

Each article in this issue is accompanied by a list of materials available from Aldrich® Materials Science. Please contact us at *matsci@sial.com* if you need any material that you cannot find in our catalog, or would like a custom grade for your development work. We welcome your new product requests and suggestions as we continue to grow our lithography/patterning material offer.

About Our Cover

The fabrication and testing of most electronic semiconductor-based devices is currently carried out in commercialized, expansive facilities employing highly automated photolithographic techniques where features down to 45 nm and beyond are not uncommon. This top-down approach in creating integrated circuits using filters and photo masks is considered standard practice; however, bottom-up self-assembly approaches that can further miniaturize features below 10 nm are now being included. The basic concept of using UV light and a mask to transcribe features onto an electronic substrate, such as single crystal silicon, is shown.

Your Materials Matter.

Jeff Thurston, President
Aldrich Chemical Co., Inc.

Do you have a compound that you wish Sigma-Aldrich® could list to help materials research? If it is needed to accelerate your research, it matters—please send your suggestion to matsci@sial.com and we will be happy to give it careful consideration.

Professor Paul Nealey of University of Wisconsin-Madison kindly suggested that we offer 4-vinylbenzocyclobutene (VBCB – **Aldrich Prod. No. 733377**) as a product in our catalog. This molecule is designed for the preparation of ultra-thin, crosslinkable films to modify solid surfaces without reliance on specific chemistries.[1] The vinyl component readily co-polymerizes with various monomers and upon subsequent heating at 250 °C the cyclobutene ring opens to produce a diene, which is capable of dimerization. This leads to the formation of a cross-linked polymer film, which forms a robust coating on the surface and is resistant to common solvents. In addition, this monomer has also shown promise in the synthesis of polymers suitable as dielectric materials for microelectronics applications. Polymer blends containing the VBCB unit and thermoplastic elastomers give rise to materials that maintain a high glass transition temperature (T_g) with only a slight decrease in thermal stability.[2]
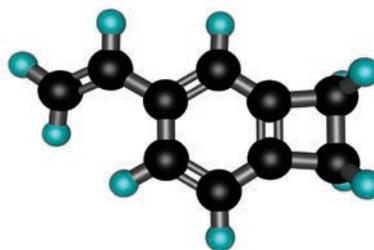
4-Vinylbenzocyclobutene

VBCB
[99717-87-0] $C_{10}H_{10}$ FW 130.19
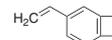
733377-1G	1g

References

(1) Ryu, D. Y.; Shin, K.; Drockenmuller, E.; Hawker, C. J.; Russell, T. P. *Science* **2005**, *308*, 236-239.
(2) So, Y.-H.; Hahn, S. F.; Li, Y.; Reinhard, M. T. *J. Polym. Sci., Part A: Polym. Chem.* **2008**, *46*, 2799-2806

Nanopatterning and Lithography Materials Featured in this Issue

For questions, product data, or new product suggestions, please contact Aldrich Materials Science at *matsci@sial.com*.

1

Hexafluoroalcohol-functionalized Methacrylate Monomers for Lithographic/Nanopatterning Materials

Daniel P. Sanders, Ratnam Sooriyakumaran, Richard A. DiPietro*
IBM Almaden Research Center, San Jose, CA
*Email: dipietro@almaden.ibm.com

Introduction

To keep pace with Moore's Law, there is a continuing need in the semiconductor industry to achieve higher circuit density in micro-electronic devices. The principle means of defining high resolution circuitry found in today's semiconductor devices is the patterning of radiation-sensitive polymeric films using the lithographic process shown in **Figure 1**.[1,2]
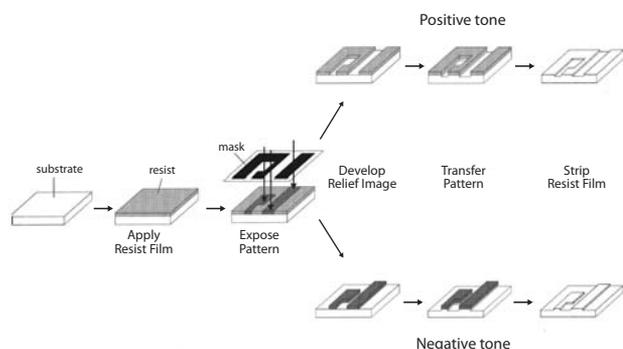
Figure 1. The lithographic process can be used to generate patterns using a positive or negative tone resist.[1]

In the first step, a layer of photosensitive material (a photoresist) is spin-applied to a desired film thickness on a silicon wafer. The film is exposed through a mask and a series of lenses with an appropriate wavelength of ultraviolet radiation. The photoresist formulation generally comprises a polymer that incorporates a "solubility switch", a functionality that enables the solubility characteristics (e.g., the dissolution rate) of the polymer film to be changed via photochemical means.[3-5] Modern chemically amplified photoresists are formulated with a photoacid generator (PAG) which, upon exposure to high energy radiation, decomposes to produce a strong acid. This acid catalyzes chemical reactions, such as the cleavage of acid-labile protecting groups on the photoresist polymer or the formation of chemical crosslinks between photoresist polymer chains, which alter the dissolution properties of the photoresist.[3-5] Selectively removing (developing) the exposed material (a positive-tone resist) or the unexposed material (a negative-tone resist) using a developing solvent results in the transformation of the diffuse latent image into a rectified photoresist pattern. Finally, the photoresist pattern can be subsequently transferred into the underlying substrate by a reactive ion etch process, for example.

Important Properties of Lithographic Patterning Materials

In optical lithography, the ultimate achievable resolution is a function of the wavelength of the incident radiation according to the Rayleigh equation:

$$R = \frac{k_1 \lambda}{NA} \qquad (1)$$

where R is the resolution (e.g., minimum critical dimension), λ is the wavelength of the incident radiation, NA is the numerical aperture of the lens system, and k_1 is a process-dependent factor typically between 0.5 and 0.25.[1,2] In order to achieve smaller feature sizes, industry has traditionally moved to shorter wavelengths of light, often requiring redesign of photoresists to accommodate the new radiation wavelength.[1-5] In particular, the non-radiation-sensitive components of the formulation must be relatively transparent to avoid non-productive attenuation of the incident radiation. For example, photoresist polymers based on 4-hydroxystyrene (polyhydroxystyrene – PHS) and its copolymers are widely used with 248 nm radiation due to their advantageous optical, dissolution, and etch properties; however, these aromatic polymers absorb heavily at 193 nm. Subsequently, new photoresists based on acrylate, methacrylate, or cyclic olefin polymers were developed which are transparent at 193 nm. While a compre-hensive discussion of chemically-amplified photoresist materials can be found elsewhere,[3-5] one important parameter to be considered in the design of new photoresist materials is the dissolution behavior of the photoresist. The aforementioned hydroxystyrene-based materials used in 248 nm imaging tend to dissolve very uniformly in industry standard 0.26N aqueous tetramethylammonium hydroxide (TMAH) developer without swelling or excess thinning in the unexposed regions (dark loss). In contrast, the aforementioned 193 nm photoresist polymer platforms which use carboxylic acid groups as solubilizing functionalities often show nonlinear dissolution and often exhibit significant swelling during the initial stages of development. This has made the development of photoresists based on these materials quite challenging, particularly for negative-tone formulations.

Beneficial Properties of HFA Methacrylate Polymers

Alternatively, photoresist materials featuring highly fluorinated alcohols as a solubilizing functionality in place of a phenolic group have been developed.[3,6] In particular, the conjugate bases of hexafluoroalcohols (HFAs) (such as 1,1,1,3,3,3-hexafluoro-2-propanol, Aldrich Prod. No. 325244) are inductively stabilized by the heavily electron-with-drawing trifluoromethyl groups such that the alcohols display pK_a values similar to that of the aforementioned phenolic materials (pK_a ~11).[7]

HFA-functionalized polymers have been designed for use in 248 nm, 193 nm, and 157 nm lithography; however, lithographic materials based on HFA-functionalized methacrylate monomers (see Figure 2) have been advantageously employed in 193 nm dry and immersion lithography due to their linear dissolution behavior with little swelling.[3,6,8-10]
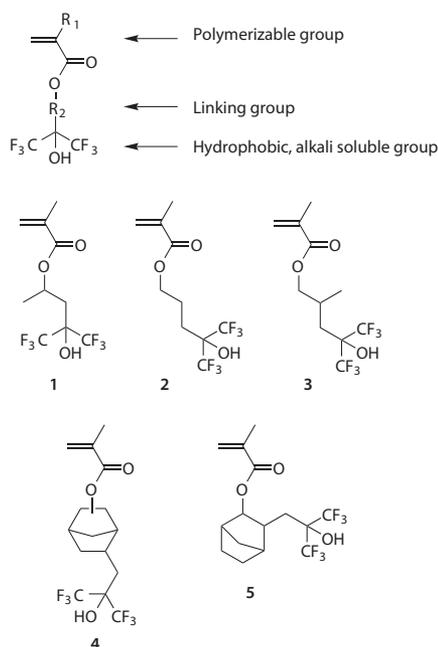
Figure 2. HFA-functional methacrylate monomers designed for use in 193 nm lithography.

This is in contrast to the dissolution behavior of lithographic materials based solely on carboxylic acids. For example, in Figure 3 the methacrylic acid copolymer shows significant swelling during the initial stages of development [evidenced by the increase in thickness and shift in resistance as measured by a quartz crystal microbalance (QCM)] during development, while the HFA-based poly(1) shows linear dissolution.
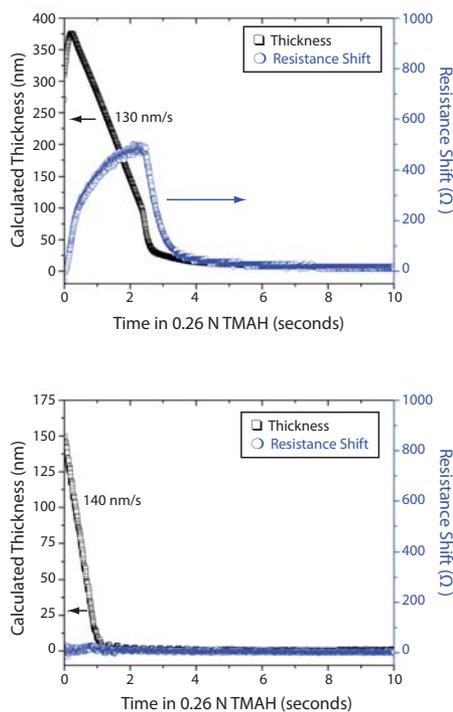
Figure 3. Dissolution behavior as determined by QCM of a methacrylic acid copolymer Top: poly(methyl methacrylate-co-methacrylic acid) 4:1 (Aldrich Prod. No. 376914). Bottom: HFA methacrylate polymer, made using monomer (1).

Properties of Representative HFA Methacrylate Homopolymers

A series of homopolymers were prepared using AIBN-initiated free-radical polymerization (Aldrich Prod. No. 441090) of the HFA methacrylates shown in Figure 2 and their properties are listed in Table 1. Since lower molecular weight polymers exhibit higher dissolution rates, low molecular weight (<10 kDa) polymers were produced using 1-dodecanethiol (Aldrich Prod. No. 471364) as a chain transfer agent (CTA). In the absence of CTAs, higher molecular weights are readily achievable. The properties of HFA methacrylate polymers can be tuned by modifying their molecular weights, changing the structure of the linking group, or by copolymerization with other comonomers.[11,12] In particular, HFA methacrylates with polycyclic groups (such as 4 and 5) can be used as comonomers in photoresist polymers where the polycyclic groups serve to increase oxygen reactive ion etch resistance.[6,8-10] By contrast, monomer 1 with its short, branched linking group has found to be particularly useful in immersion lithography applications where high water contact angles and TMAH dissolution rates are more important.[12-14]

Table 1. HFA methacrylate homopolymers and their properties as they relate to UV lithography.

Polymer[a]	Mn [g/mol]	PDI	T_g	Dissolution Rate in TMAH 0.26N	0.52N	Static water contact angle	Static, advancing contact angle[b]	Static, receding contact angle[b]
Poly(1)	4220	1.56	89 °C	125 nm/s	1010 nm/s	83°	87°	66°
Poly(2)	6130	1.14	66 °C	990 nm/s	-	71°	77°	50°
Poly(3)	5920	1.56	55 °C	245 nm/s	-	75°	83°	58°
Poly(4)	9290	1.32	159 °C	~0 nm/s	3.2 nm/s	77°	81°	65°
Poly(5)	11000	1.26	148 °C	~0 nm/s	~0 nm/s	86°	86°	74°

[a]Prepared from Monomers 1-5 in Figure 2, respectively, using AIBN-initiated free radical polymerization.
[b]Measured using a tilting table contact angle goniometer.

For questions, product data, or new product suggestions, please contact Aldrich Materials Science at *matsci@sial.com*.

ALDRICH® Materials Science

3

Applications of HFA Methacrylates in Lithographic/Nanopatterning Materials

193 nm Photoresist Materials

Figure 4 shows the dissolution behavior (as measured using a quartz crystal microbalance) of a 248 nm photoresist and a 193 nm photoresist as a function of exposure dose using a 254 nm Hg/Xe lamp. In comparison with the hydroxystyrene-based 248 nm photoresist, the partially deprotected 193 nm photoresist produced at intermediate dosages displays significant swelling in TMAH developer. With respect to imaging performance, such swelling can lead to enhanced line edge roughness (LER), line width roughness (LWR), and decreased process latitude. In contrast, a photoresist incorporating monomer 4 (**Figure 4**, HFA resist) displays similar dissolution behavior as the polyhydroxystyrene-based 248 nm photoresist.[8,9]
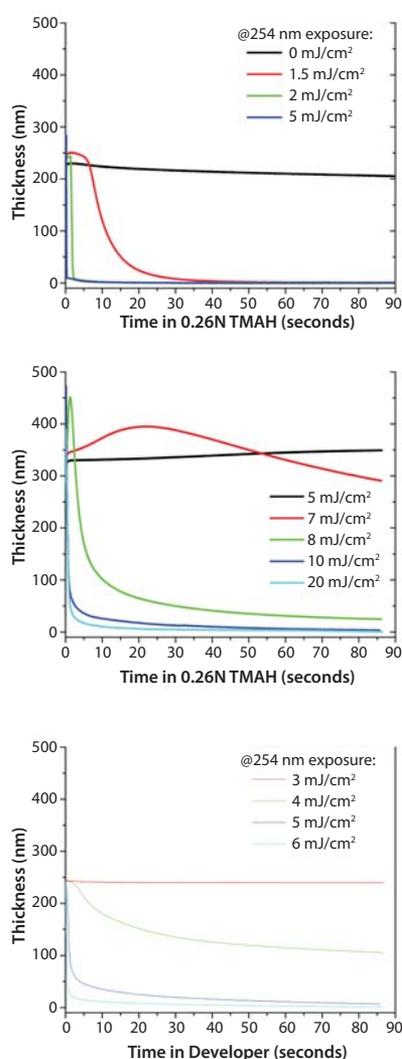
Figure 4. Dissolution behavior of a **Top:** 248 nm photoresist, **Middle:** 193 nm photoresist and **Bottom:** HFA-containing 193 nm photoresist based on poly(t-butyl methacrylate-co-**4**).

Alkali-soluble Topcoats for 193 nm Water Immersion Lithography

In place of 157 nm lithography, the semiconductor industry has turned to immersion lithography to extend the capabilities of 193 nm lithography.[15] Immersion lithography involves placing an immersion fluid with a refractive index greater than air between the final lens element of the exposure system and the photoresist. The use of an immersion fluid enables the development of imaging systems with numerical apertures greater than 1 (so-called hyper-NA imaging systems) and, for any given NA, increases the available depth of focus and thereby improves process latitude.[15] At 193 nm, water is the ideal immersion fluid due to its high transparency, ready availability in labs with high purity at low cost, and good thermal, viscosity, and surface tension properties. Since immersion lithography changes only the effective wavelength (λ_o/n) and not the vacuum wavelength (λ_o) of the incident radiation, the large body of existing 193 nm technology (source lasers, optical materials, photoresist and anti-reflective materials) can be reused.

The introduction of immersion lithography has required the development of improved photoresist materials to accommodate direct contact with the immersion fluid.[16,17] As shown in **Figure 5**, immersion fluids can have adverse effects on the photoresist by extracting key photoresist components such as photoacid generators thereby degrading imaging performance and potentially contaminating the exposure tool.[16-18] To overcome these problems, protective polymeric topcoats may be employed to reduce extraction of photoresist components into the immersion fluid and, thereby, protect the immersion scanner and retain photoresist patterning performance.[16] Topcoat materials are designed to exhibit high receding contact angles with water, in order to enable rapid scanning of the wafer without film pulling (i.e., leaving a trail of film or droplets behind the receding meniscus of the immersion fluid).[19] Since these residual water droplets induce defects in the final lithographically printed features, the receding contact angle of the immersion fluid with the topcoat effectively determines the maximum wafer scan rate and tool throughput.[16-17,19]
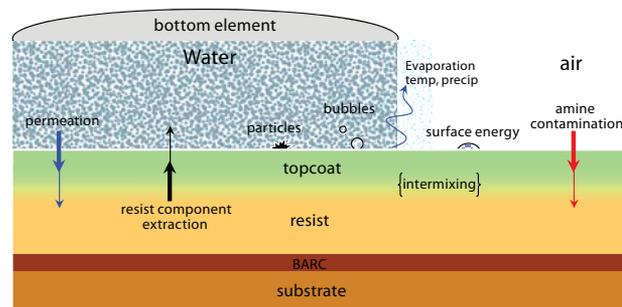
Figure 5. A graphical representation of key material interactions in immersion lithography.

HFA methacrylate polymers are particularly advantageous for use in topcoat applications due to their unique combination of high, receding water contact angles and moderate TMAH dissolution rates (as compared to polymers based on alternative alkali-soluble groups such as carboxylic acid).[12-14,16,20] In addition, HFA methacrylate polymers have high solubility in alcoholic casting solvents and therefore can be spun-cast on top of photoresists with minimal interdiffusion.

Polymer **6** (in **Figure 6**), in particular, exhibits an ideal balance of contact angle and dissolution rate performance from which to begin designing a topcoat material.[12,16] Copolymerization with fluoroalkyl methacrylates such as 1,1,1,3,3,3-hexafluoroprop-2-yl methacrylate can be used to increase contact angles at the expense of dissolution rate (see polymer **7**, **Figure 6**). Alternatively, comonomers containing strongly acidic groups can be used (for example, 2-acrylamido-2-methyl-1-propanesulfonic acid in polymer **8**, **Figure 6**) to tune the topcoat-photoresist interactions and improve pattern profiles (e.g., reduce t-topping) albeit at the expense of water contact angles.[14]
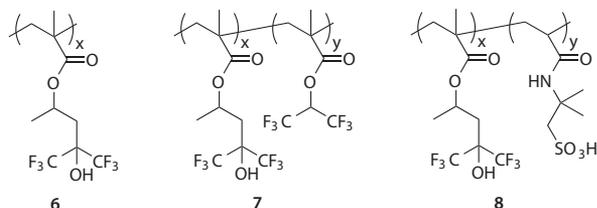
Figure 6. Example topcoat polymers for 193 nm immersion lithography.

Surface-active Polymer Additives for 193 nm Water Immersion Lithography

While protective topcoats are often used in water immersion lithography, a topcoat-based lithographic process requires additional process steps and material cost as compared to conventional dry lithography. Alternatively, topcoat-free photoresists have been developed for immersion lithography in which small quantities of surface-active fluoropolymer additives segregate to the photoresist surface during film formation to minimize photoacid generator leaching and control immersion fluid-photoresist interactions.[16] These topcoat-free photoresists are intended to enable the high throughput and low defectivity characteristic of topcoat-based immersion lithography processes without the extra materials and process costs.

A wide variety of surface-active fluoropolymer additives have been developed for topcoat-free immersion photoresists.[16] In general, most additives fall into one of two categories: developer soluble (topcoat type) and switchable (resist type). Developer soluble additives require many of the same material properties that have made HFA methacrylates useful for immersion topcoats, including high water contact angles and moderate dissolution rates in aqueous base developer. Switchable additives are essentially fluorinated photoresists themselves that have been optimized for their surface properties. While many fluorinated surface-active resins can impart good water contact angles during patterning, HFA methacrylate materials undergo a pH-induced transition from hydrophobic to hydrophilic in the presence of an alkaline developer thereby ensuring good developer wetting during development.[12,16] For example, an unexposed topcoat-free photoresist formulated with the simple fluorinated polymer additive **9** exhibits high receding contact angles with both water and aqueous TMAH developer, whereas an analogous topcoat-free photoresist formulated with the HFA-based additive polymer **10** displays a much reduced contact angle with TMAH developer (see **Figure 7**).
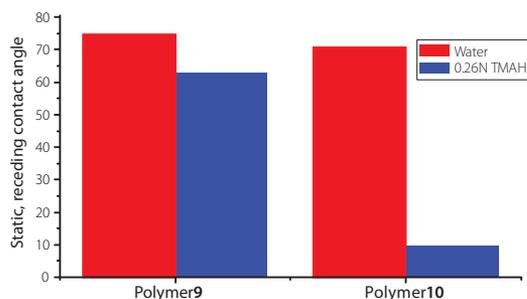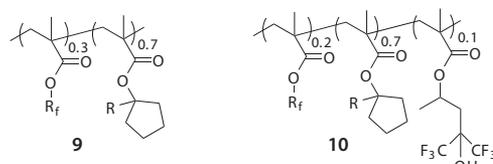
Figure 7. Static, receding contact angles of water and TMAH developer on topcoat-free photoresists formulated with the polymeric additives shown.

Impact

Leading-edge, positive-tone photoresists based on HFA methacrylates have had a major impact within IBM for the commercial manufacturing of several generations of chips produced using 193 nm dry lithography. This chemistry has also played an enabling role in the rapid introduction of immersion lithography into high volume manufacturing through their incorporation into immersion topcoats and topcoat-free photoresists used throughout the industry. The flexibility inherent in the HFA-MA monomers allows the materials designer great freedom in the precise tuning of polymer properties and performance in microelectronics as well as applications outside the semiconductor industry.

References

(1) Wallraff, G. M.; Hinsberg, W. D. *Chem. Rev.* **1999**, *99*, 1801.
(2) Mack, C. *Fundamental Principles of Optical Lithography: The Science of Microfabrication.* Wiley: West Sussex, England, **2008**.
(3) Ito, H. *Adv. Polym. Sci.* **2005**, *172*, 37.
(4) MacDonald, S. A.; Willson, C. G.; Fréchet, J. M. J. *Acc. Chem. Res.* **1994**, *27*, 153.
(5) Reichmanis, E.; Houlihan, F. M.; Nalamasu, O.; Neenan, T. X. *Chem. Mater.* **1991**, *3*, 394.
(6) Ito, H.; Truong, H. D.; Allen, R. D.; Li, W.; Varanasi, P. R.; Chen, K.-J.; Khojasteh, M.; Huang, W.-S.; Burns, S. D.; Pfeiffer, D. *Polym. Adv. Technol.* **2006**, *17*, 104.
(7) Gandler, J. R.; Jencks, W. P. *J. Am. Chem. Soc.* **1982**, *104*, 1937.
(8) Varanasi, P. R.; Kwong, R. W.; Khojastech, M.; Patel, K.; Chen, K.-J.; Li, W.; Lawson, M. C.; Allen, R. D.; Sooriyakumaran, R.; Brock, P.; Sundberg, L. K.; Slezak, M.; Dabbagh, G.; Liu, Z.; Nishimura, Y.; Chiba, T.; Shimokawa, T. *J. Photopolym. Sci. Technol.* **2005**, *18*, 381.
(9) Varanasi, P. R.; Kwong, R. W.; Khojastech, M.; Patel, K.; Chen, K.-J.; Li, W.; Lawson, M. C.; Allen, R. D.; Sooriyakumaran, R.; Brock, P.; Sundberg, L. K.; Slezak, M.; Dabbagh, G.; Liu, Z.; Nishimura, Y.; Chiba, T.; Shimokawa, T. *Proc. SPIE* **2005**, *5753*, 131.
(10) Patel, K.; Lawson, M.; Varanasi, P.; Medeiros, D.; Wallraff, G.; Brock, P.; DiPietro, R.; Nishimura, Y.; Chiba, T.; Slezak, M. *Proc. SPIE* **2004**, *5376*, 94.
(11) Allen, R. D.; Breyta, G.; Brock, P.; DiPietro, R.; Sanders, D.; Sooriyakumaran, R.; Sundberg, L. K. *J. Photopolym. Sci. Technol.* **2006**, *19*, 569.
(12) Sanders, D. P.; Sundberg, L. K; Sooriyakumaran, R.; Brock, P. J.; DiPietro, R. A.; Truong, H. D.; Miller, D. C.; Lawson, M. C.; Allen, R. D. *Proc. SPIE* **2007**, *6519*, 651904.
(13) Allen, R. D.; Brock, P. J.; Sundberg, L.; Larson, C. E.; Wallraff, G. M.; Hinsberg, W. D.; Meute, J.; Shimokawa, T.; Chiba, T.; Slezak, M. *J. Photopolym. Sci. Technol.* **2005**, *18*, 615.
(14) Khojasteh, M.; Popova, I.; Varanasi, P. R.; Sundberg, L.; Robinson, C.; Corliss, D.; Lawson, M.; Dabbagh, G.; Slezak, M.; Colburn, M.; Petrillo, K. *Proc. SPIE* **2007**, *6519*, 651907.
(15) Lin, B. J. *J. Microlith., Microfab., Microsyst.* **2004**, *3*, 377.
(16) Sanders, D. P. *Chem. Rev.* **2010**, *110*, 321.
(17) Wei, Y.; Brainard, R. L. *Advanced Processes for 193-nm Immersion Lithography* SPIE Press, Bellingham, WA, 2009.
(18) Wallraff, G. M.; Larson, C. E.; Breyta, G.; Sundberg, L.; Miller, D.; Gil, D.; Petrillo, K.; Person, W. *Proc. SPIE* **2006**, *6153*, 61531M.
(19) Schuetter, S. D.; Shedd, T. A.; Nellis, G. F. *J. Micro/Nanolith. MEMS MOEMS* **2007**, *6*, 023003.
(20) Sundberg, L. K.; Sanders, D. P.; Sooriyakumaran, R.; Brock, P. J.; Allen, R. D. *Proc. SPIE* **2007**, *6519*, 65191Q.

For questions, product data, or new product suggestions, please contact Aldrich Materials Science at *matsci@sial.com*.

5

HFA-MA Monomers for Lithographic/Nanopatterning Materials

For a complete list of available products, please visit *aldrich.com/lithography*

Name	Structure	Purity	Prod. No.
1,1,1-Trifluoro-2-trifluoromethyl-2-hydroxy-4-methyl-5-pentyl methacrylate		>97%	733695-1G 733695-5G
2-[(1′,1′,1′-Trifluoro-2′-trifluoromethyl-2′-hydroxy)prop-yl]-3-norbornyl methacrylate		>97%	733660-1G 733660-5G
1,1,1-Trifluoro-2-trifluoromethyl-2-hydroxy-5-pentyl methacrylate		*	737895-5G
1,1,1-Trifluoro-2-trifluoromethyl-2-hydroxy-4-pentyl methacrylate		*	737909-5G
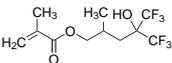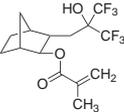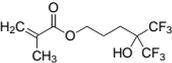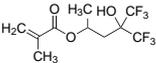
*For updated purities, please visit the Sigma-Aldrich website at sigma-aldrich.com

Monomers for UV Lithography

For a complete list of available products, please visit *aldrich.com/lithography*

Name	Structure	Purity	Prod. No.
3-Oxabicyclo[3.1.0]hexane-2,4-dione		98%	391174-1G
Bicyclo[2.2.1]hepta-2,5-diene, 2,5-Norbornadiene; NBD		98%	B33803-5ML B33803-100ML B33803-500ML
7-*tert*-Butoxy-2,5-norbornadiene		96%	446432-1G
exo-5-Norbornenecarboxylic acid, NC		97%	718149-1G 718149-5G
cis-5-Norbornene-*endo*-2,3-dicarboxylic acid, NDC		98%	216704-5G 216704-25G
5-Norbornene-2-*endo*,3-*exo*-dicarboxylic acid, NDC		97%	460036-5G
5-Norbornene-2,2-dimethanol, NDM		98%	152188-1G
5-Norbornene-2-*endo*,3-*endo*-dimethanol, NDM		98%	460044-1G 460044-5G
5-Norbornene-2-*exo*,3-*exo*-dimethanol, NDM		97%	460052-5G
exo-2,3-Epoxynorbornane, ENB		97%	117803-5G 117803-25G
cis-5-Norbornene-*exo*-2,3-dicarboxylic anhydride		95%	548006-5G

aldrich.com TO ORDER: Contact your local Sigma-Aldrich office (see back cover) or visit **aldrich.com/matsci**.

Name	Structure	Purity	Prod. No.
cis-5-Norbornene-endo-2,3-dicarboxylic anhydride		97%	247634-5G 247634-25G
N-Hydroxy-5-norbornene-2,3-dicarboxylic acid imide, HONB		97%	226378-50G
1,4,5,6,7,7-Hexachloro-5-norbornene-2,3-dicarboxylic anhydride		97%	103268-1KG
Methyl-5-norbornene-2,3-dicarboxylic anhydride		90%	235431-5G 235431-250G 235431-1KG
Isobornyl methacrylate, IBMA		-	392111-100ML 392111-500ML 392111-1L
Isobornyl acrylate, IBA		-	392103-100ML 392103-500ML 392103-1L
Tetrahydrofurfuryl acrylate, TFMA		-	408271-100ML
[Tris(dimethylphenylphosphine)](2,5-norbornadiene)rhodium(I) hexafluorophosphate		97%	337501-100MG 337501-500MG
1,3-Adamantanediacetic acid, H2ADA		97%	146226-1G 146226-5G
1,3-Adamantanedicarboxylic acid, ADC		98%	340820-1G 340820-5G
Dimethyl 1,3-adamantanedicarboxylate, DMADC		98%	340839-1G 340839-5G

Fluorinated Monomers for UV Lithography

For a complete list of available products, please visit *aldrich.com/lithography*

Name	Structure	Purity	Prod. No.
2-(Trifluoromethyl)acrylic acid, TFMAA		98%	369144-1G 369144-5G
2,2,2-Trifluoroethyl acrylate, TFEA		99%	297720-5G 297720-25G
1,1,1,3,3,3-Hexafluoroisopropyl acrylate, HFiPA		99%	367656-5G
1,1,1,3,3,3-Hexafluoroisopropyl methacrylate, HFiPMA		99%	367664-1G 367664-5G
2,2,3,3,3-Pentafluoropropyl acrylate, PFPA		98%	470961-5ML 470961-25ML

For questions, product data, or new product suggestions, please contact Aldrich Materials Science at *matsci@sial.com*.

ALDRICH Materials Science

7

Name	Structure	Purity	Prod. No.
2,2,3,4,4,4-Hexafluorobutyl acrylate, HFBA		95%	474452-25ML
2,2,3,4,4,4-Hexafluorobutyl methacrylate, HFBMA		98%	371971-5G 371971-25G
2,2,3,3,4,4,4-Heptafluorobutyl acrylate, HFBA		97%	443751-5ML
2,2,3,3,4,4,4-Heptafluorobutyl methacrylate, HFBMA		97%	444006-1G 444006-5G
2,2,3,3,4,4,5,5-Octafluoropentyl acrylate, OFPA		97%	474401-25ML
2,2,3,3,4,4,5,5-Octafluoropentyl methacrylate, OFPMA		98%	470988-25ML
2,2,3,3,4,4,5,5,6,6,7,7-Dodecafluoroheptyl acrylate, DFHA		95%	474428-5ML
3,3,4,4,5,5,6,6,7,7,8,8,8-Tridecafluorooctyl acrylate, TFOA	$CH_2CH_2(CF_2)_5CF_3$	97%	474347-5ML 474347-25ML
1H,1H,2H,2H-Perfluorodecyl acrylate	$OCH_2CH_2(CF_2)_7CF_3$	97%	474487-5ML 474487-25ML
3,3,4,4,5,5,6,6,7,7,8,8,9,9,10,10,10-Heptadecafluorodecyl methacrylate, HDFDMA	$CH_2CH_2(CF_2)_7CF_3$	97%	474223-25ML
3,3,4,4,5,5,6,6,7,7,8,8,9,9,10,10,11,11,12,12,12-Heneicosa-fluorododecyl acrylate	$CF_2(CF_2)_8CF_3$	96%	474355-5G
Zonyl® TM fluoromonomer		–	421480-50ML
Epifluorohydrin		98%	E1101-1G
Hexafluoropropylene oxide		98%	323640-50G 323640-300G
Glycidyl 2,2,3,3-tetrafluoropropyl ether		97%	474150-25ML
Glycidyl 2,2,3,3,4,4,5,5-octafluoropentyl ether		96%	474169-5ML
(2,2,3,3,4,4,5,5,6,6,7,7,8,8,9,9,9-Heptadecafluorononyl) oxirane	$CF_3(CF_2)_7CH_2$	96%	474088-5ML 474088-25ML
[2,2,3,3,4,4,5,5,6,6,7,7,8,9,9,9-Hexadecafluoro-8-(trifluoromethyl)nonyl]oxirane	F_3C $CF_2(CF_2)_5CH_2$	96%	474134-25ML
Glycidyl 2,2,3,3,4,4,5,5,6,6,7,7,8,8,9,9-hexadecafluoro-nonyl ether	$OCH_2(CF_2)_6CF_2$	96%	474185-5ML
N-Hydroxy-5-norbornene-2,3-dicarboximide perfluoro-1-butanesulfonate		≥99% trace metals basis	531111-1G 531111-5G

Photoacid Generators (PAGs)

For a complete list of available products, please visit *aldrich.com/pags*

Name	Structure	$\lambda_{abs}/\lambda_{max}$	Prod. No.
Triphenylsulfonium triflate, TPST		233 nm	526940-1G 526940-5G
Triphenylsulfonium perfluoro-1-butanesufonate		-	531057-1G 531057-5G
(4-Methoxyphenyl)diphenylsulfonium triflate		260 nm	526967-5G
(4-Phenoxyphenyl)diphenylsulfonium triflate		256 nm	526975-1G-A 526975-5G-A
(4-Phenylthiophenyl)diphenylsulfonium triflate		298 nm	527009-1G 527009-5G
Tris(4-*tert*-butylphenyl)sulfonium triflate		201 nm	531030-1G
Tris(4-*tert*-butylphenyl)sulfonium perfluoro-1-butane-sulfonate		-	531073-1G 531073-5G
Triarylsulfonium hexafluorophosphate salts, mixed		-	407216-25ML 407216-100ML
Diphenyliodonium hexafluorophosphate, DPIHFP		-	548014-5G 548014-25G
Diphenyliodonium nitrate, DPIN		203 nm 226 nm	127396-25G
Diphenyliodonium triflate, DPIT		-	530972-1G
Diphenyliodonium *p*-toluenesulfonate, DPIpTS		222 nm	530980-1G 530980-5G
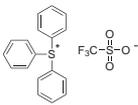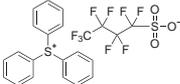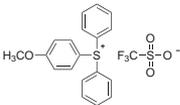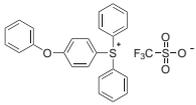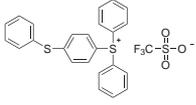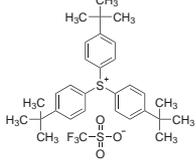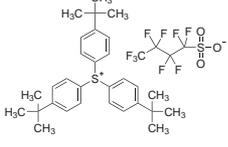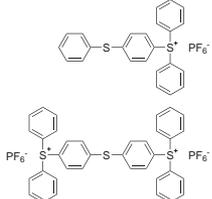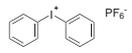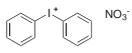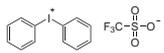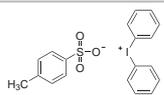
For questions, product data, or new product suggestions, please contact Aldrich Materials Science at *matsci@sial.com*.

ALDRICH® Materials Science

9

Name	Structure	$\lambda_{abs}/\lambda_{max}$	Prod. No.
Bis(4-*tert*-butylphenyl)iodonium triflate, DtBPIT		-	530999-1G 530999-5G
Bis(4-*tert*-butylphenyl)iodonium perfluoro-1-butane-sulfonate		-	531014-1G 531014-5G
Bis(4-*tert*-butylphenyl)iodonium *p*-toluenesulfonate		202 nm	531006-1G 531006-5G
2-(4-Methoxystyryl)-4,6-bis(trichloromethyl)-1,3,5-triazine		379 nm	530964-5G-A
N-Hydroxynaphthalimide triflate, HNT; NHN-TF		-	531081-1G
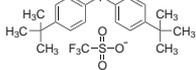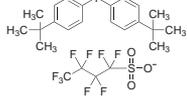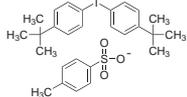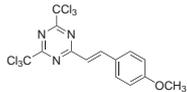
Substrates for Lithography

For a complete list of available products, please visit *aldrich.com/substrates*

Name	Orientation	Semiconductor Type	Dopant	Dimensions	Prod. No.
Silicon, wafer (single side polished)	(100)	N	undoped	diam. × thickness 2 in. × 0.5 mm	646687-1EA 646687-5EA
	(100)	-	undoped	diam. × thickness 3 in. × 0.5 mm	647535-1EA 647535-5EA
	(100)	N	phosphorus	diam. × thickness 2 in. × 0.5 mm	647780-1EA 647780-5EA
	(100)	N	phosphorus	diam. × thickness 3 in. × 0.5 mm	647802-1EA
	(100)	P	boron	diam. × thickness 2 in. × 0.5 mm	647675-5EA 647675-1EA
	(100)	P	boron	diam. × thickness 3 in. × 0.5 mm	647764-1EA 647764-5EA
	(111)	N	undoped	diam. × thickness 2 in. × 0.5 mm	647101-1EA 647101-5EA
	(111)	N	undoped	diam. × thickness 3 in. × 0.5 mm	647543-1EA 647543-5EA
	(111)	N	phosphorus	diam. × thickness 2 in. × 0.5 mm	647799-1EA 647799-5EA
	(111)	N	phosphorus	diam. × thickness 3 in. × 0.5 mm	647810-5EA 647810-1EA
	(111)	P	boron	diam. × thickness 2 in. × 0.5 mm	647705-1EA
	(111)	P	boron	diam. × thickness 3 in. × 0.5 mm	647772-5EA
Silicon dioxide, crystalline	(0001)	-	undoped	L × W × thickness 10 mm × 10 mm × 0.5 mm	634867-5EA
Magnesium oxide, (single crystal substrate)	(100)	-	undoped	L × W × thickness 10 mm × 10 mm × 0.5 mm	634646-1EA
	(110)	-	undoped	L × W × thickness 10 mm × 10 mm × 0.5 mm	634700-1EA
	(111)	-	undoped	L × W × thickness 10 mm × 10 mm × 0.5 mm	634697-1EA
Gallium antimonide, (single crystal substrate)	(100)	-	undoped	diam. × thickness 2 in. × 0.5 mm	651478-1EA
Gallium arsenide, (single crystal substrate)	(100)	-	undoped	diam. × thickness 2 in. × 0.5 mm	651486-1EA
Gallium phosphide, (single crystal substrate)	(111)	-	undoped	diam. × thickness 2 in. × 0.5 mm	651494-1EA
Titanium(IV) oxide, rutile, (single side polished), (single crystal substrate)	(001)	-	undoped	L × W × thickness 10 mm × 10 mm × 0.5 mm	635057-1EA
	(100)	-	undoped	L × W × thickness 10 mm × 10 mm × 0.5 mm	635049-1EA
	(110)	-	undoped	L × W × thickness 10 mm × 10 mm × 0.5 mm	635065-1EA

Silicon Nanowires

Aldrich® Materials Science is proud to offer a selection of high-purity silicon nanowires for use in a variety of high-technology applications. The nanowires are available monodispersed either undoped or doped (p-type) as well as polydispersed with varying lengths. As analogs to carbon nanotube materials, silicon nanowires are beginning to be realized for applications including field-effect transistors,[1] photovoltaics,[2] sensors,[3] lithium batteries[4] and catalysts.[5] They can be assembled or aligned onto a number of flexible or transparent substrates using both established and cutting-edge methods. One such refined method includes the alignment of individual silicon nanowires between more than 16,000 electrodes using a balanced combination of dielectrophoretic forces and uniform fluid flow.[6]

Silicon nanowires are also excellent candidates for biologically related applications such as tissue-engineering, biosensors and drug/gene-delivery because they are environmentally friendly, biocompatible and simple to modify.[7] The nanoscale diameter and the high aspect ratio of silicon nanowires allow them to be readily accessible to the interior of living cells, which opens up the study of intracellular molecular level interactions.[8] Their compatibility with conventional silicon microtechnology, together with reliable quality and consistent availability from Aldrich Materials Science will help accelerate the adoption of these high-performance materials. Together with the availability of gold nanowires, more effective development of nanowire-based technologies is expected.

Monodispersed Silicon Nanowires*

Prod. No.	Doping	Approx. Dimen. (D × L)	Dispersant	Conc.	Purity
730866	Undoped	150 nm × 20 μm	Isopropyl Alcohol	~1 μg/mL	>99% Si
730874	P-I-P	150 nm × 20 μm	Isopropyl Alcohol	~1 μg/mL	>99% Si

Polydispersed Silicon Nanowires*

Prod. No.	Doping	Approx. Dimen. (D × L)	Form	Purity
731498	Undoped	40 nm × 1–20 μm	Powder	>99% Si

Gold Nanowires

Prod. No.	Approx. Dimen. (D × L)	Dispersant	Concentration
716944	30 nm × 45 μm	Water	60 μg/mL
716952	30 nm × 60 μm	Water	50 μg/mL
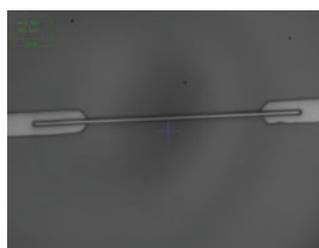
Figure 1. A single Si nanowire junction
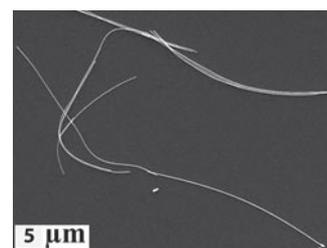
Figure 2. An SEM image of gold nanowires

References

(1) Duan, X.; Niu, C.; Sahi, V.; Chen, J.; Parce, J. W.; Empedocles, S.; Goldman, J. *Nature* **2003**, *425*, 274-278.
(2) Zhu, J.; Cui, Y. *Nat. Mater.* **2010**, *9*, 183–184.
(3) Fang, C.; Agarwal, A.; Widjaja, E.; Garland, M. V.; Wong, S. M.; Linn, L.; Khalid, N. M.; Salim, S. M.; Balasubramanian, N. *Chem. Mater.* **2009**, *21*, 3542–3548.
(4) Peng, K. Q.; Jie, J. S.; Zhang, W. J.; Lee, S. T. *Appl. Phys. Lett.* **2008**, *93*, 033105.
(5) Tsang, C. H. A.; Liu, Y.; Kang, Z. H.; Ma, D. D. D.; Wong, N. B.; Lee, S. T. *Chem. Commun.* **2009**, *39*, 5829–5831.
(6) Freer, E. M.; Grachev, O.; Stumbo, D. P. *Nat. Nanotechnol.* **2010**, *5*, 525–530.
(7) a) Patolsky, F.; Timko, B. P.; Yu, G. H.; Fang, Y.; Greytak, A. B.; Zheng, G. F. Lieber, C. M. *Science* **2006**, *313*, 1100–1104. b) Gao, Z. Q.; Agarwal, A.; Trigg, A. D.; Singh, N.; Fang, C.; Tung, C. H.; Fan, Y.; Buddharaju, K. D.; Kong, J. M. *Anal. Chem.* **2007**, *79*, 3291–3297.
(8) Zheng, G. F.; Patolsky, F.; Cui, Y.; Wang, W. U.; Lieber, C. M. *Nat. Biotechnol.* **2005**, *23*, 1294–1301.

For a continually updated list of the latest nanomaterials, visit **aldrich.com/newnano**

* Products of NanoSys, Inc.

Inkjet Printing as a Key Enabling Technology for Printed Electronics

Ashok Sridhar[1], Thomas Blaudeck[2§], and Reinhard R. Baumann[1,2*]
[1] Department Printed Functionalities, Fraunhofer Research Institute for Electronic
Nano Systems (ENAS), Technologie-Campus 3, 09126 Chemnitz, Germany
[2] Institute for Print and Media Technology, Department of Mechanical Engineering,
Chemnitz University of Technology, 09126, Chemnitz, Germany
[§] University Linköping, Department of Science and Technology (ITN),
60174 Norrköping, Sweden
[*] Email: reinhard.baumann@mb.tu-chemnitz.de

Introduction

In the past decade, the family of digital printing technologies has evolved from being just a tool to visualize information into a generator of functionalities. The phrase 'printing beyond color' aptly sums up this transformation. While this family of printing technologies is still widely used to fulfill visual requirements, its development in the generation of functionality, especially in the field of printed electronics, has resulted in an explosion of new ideas and fabrication approaches leading to lean manufacturing. The basic premise of digital printing, namely the positioning of a liquid (ink) droplet or solid (toner) particle of microscopic volume directly correlated with the presence of information at each pixel of the image or text to be produced, enables the economic deposition of expensive materials, functional or otherwise, only on desired locations on a substrate, that is, a selective deposition.

In this article, one of the most important digital fabrication techniques, inkjet printing, is presented in detail as it is one of the key enabling technologies of printed electronics. In addition to a discussion on the classification of inkjet printing technology, various relevant aspects with respect to materials (inks, substrates) as well as respective pre-processing and post-processing steps are discussed. Finally, a selection of application examples is provided, illustrating the various possibilities of inkjet-printed electronics.

Research and development focusing on functional materials and high-tech printing equipments are ongoing, leading to new innovations on a quasi-daily basis.

Background

Conventional Printing

Printing technology is one of the foremost inventions that hastened the progress of humankind by reliable transmission, exchange and preservation of knowledge. Even though Gutenberg's invention of the letterpress with movable lead type has been in existence for over half a millennium, it has been in the past century, since the evolution of photography as basis for graphic-arts reproduction and more importantly in the past few decades since the dawn of the potent combination of printing and computerized information technology, that the range of printing technologies evolved ramifyingly, leading to their widespread utilization.[1]

Offset, gravure, screen and flexographic are the major types of *conventional printing technologies*. They typically require a printing master or a printing plate for every type of information (texts, graphics and pictures) to be reproduced. Hence, an elaborate and at times cumbersome prepress process is required before these technologies can be implemented. Once the preprocessing is complete, these technologies, with the exception of flatbed screen printing, can be used for rapid and large-scale production.

Digital Printing

Unlike conventional printing technologies, *digital printing* works without a physical, pre-manufactured master printing plate and prints without a significant impact force onto the substrate or sublayer.[2] The basic premise of digital printing is the accurate positioning of a liquid droplet or solid (toner) particle of a microscopically small volume directly correlated with the presence of information at each binary unit of the imagery to be reproduced. As a result, digital printing does not have the key disadvantages of conventional printing, viz. complex working steps, typically large financial and time investments to generate the masters and set up the process. Although digital printing can be assigned certain drawbacks especially with respect to average throughput when compared to high-end conventional printing technologies, its credit lies in the fact that it has elaborated a variety of techniques and process designs making printing accessible to a broader audience. This versatility and adaptivity explains the high integration potential of digital printing techniques into existing manufacturing lines of established industries (e.g., printed circuit board), the same way it had reached industrial print shops (for book-on-demand) or revolutionized the small office/home office sector with desktop printers. The characteristic feature of digital printing technologies can be broadly classified into two groups: (1) *direct to substrate*, which consists of printing technologies (e.g., inkjet printing and thermal transfer printing) that transfer information directly onto the printing medium, i.e., substrate, and (2) *direct to plate*, which consists of printing technologies (e.g., electrophotography and magnetography) that transfer the information onto a printing plate, which, in turn, transfers it onto the printing medium.[2]

The basic premise of digital printing, namely the presence or absence of information at each pixel of the image or text to be reproduced, enables the deposition of materials, functional or otherwise, only on desired locations on a substrate, yielding a selective and hence economic deposition.

Printed Electronics

Even though the terms *printed electronics* and *organic electronics* are sometimes used interchangeably, they need not necessarily refer to the same group of technologies. Nevertheless, they do share a lot of enabling technologies and methodologies. Strictly speaking, *printed electronics* refers to the application of printing techniques, both conventional and digital, to fabricate electronic structures, devices and circuits, no matter which functional materials (ink) and substrates are used. The only prerequisite is that the functional material must be processable from the liquid phase. In the same sense, *organic electronics* deals with the application of organic materials, e.g., conductive polymers in the fabrication of electronic structures, devices and circuits on rigid or flexible substrates. Consequently, *flexible electronics* highlights the bendable substrate made of plastic or paper. In any case, the progress of printed electronics has opened up new vistas, leading to a multitude of possibilities in conception, design, fabrication, packaging and application of electronic devices and circuits.

The additive nature of printing processes, the range of materials that can be formulated as inks, and the possibility to cater to various production scales, ranging from prototype to large-scale, are some of the key factors that enable the deployment of printing processes in electronics fabrication. While almost all printing technologies, especially the conventional ones, have been used at some point in printed electronics, screen printing and inkjet printing are dominant[3]. **Figure 1** depicts the printing technologies that are of interest to printed electronics and their characteristics.

Offset Printing
- Printed pattern defined by differences in wetting of a plane surface
- Thin layers down to 0.5 µm possible; high resolution (<20 µm)
- Dynamic viscosity of ink: 40 to 100 Pa.s

Gravure Printing
- Printed pattern defined by surface relief (recesses) of master
- Broad thickness range (~1 to 8 µm); high resolution (<20 µm)
- Dynamic viscosity of ink: 0.05 to 0.2 Pa.s

Flexographic Printing
- Printed pattern defined by surface relief (raised features) of master
- Thin layers of about 1 µm possible; high resolution (~20 µm)
- Dynamic viscosity of ink: 0.05 to 0.5 Pa.s

Screen Printing
- Printed pattern defined by openings in printing master
- Thick layers (>10 µm) possible; low resolution (~100 µm)
- Very broad dynamic viscosity range, from gravure inks to offset inks

Inkjet Printing
- Master-less; droplet size determined by nozzle diameter and waveform
- Thin layers down to 100 nm possible; moderate resolution (~50 µm)
- Dynamic viscosity of ink: 1 to 20 mPa.s

Figure 1. Printing technologies that are of interest for printed electronics and their significant characteristics.[1,3-5]

It is worthwhile to note that, apart from inkjet printing, all the other technologies listed in **Figure 1** are conventional in nature. In spite of that, the digital inkjet printing is considered a key enabling technology for printed electronics for reasons listed in the next section. The classification, specifics and requirements of inkjet technology are discussed in detail, along with application examples that illustrate the suitability of this kind of technology for printed electronics.

Inkjet Printing Technology

The inkjet printing technology produces droplets of the ink contained in the fluid channel, with diameters ranging from 10 to 150 µm,[6] which approximately corresponds to the diameter of the nozzle. The volume of the droplets is in the picoliter range. This technology is considered suitable for printed electronics due to the following reasons:

- It is a non-contact process that selectively deposits a wide range of materials onto a wide range of substrates in a drop-by-drop manner.
- The shop floor space requirements, the initial investment as well as the commissioning time to get an inkjet printing setup running are lower than most other printing technologies.
- It is suitable for a wide range of production scales, from prototyping to large-scale industrial production.
- Ink consumption and material wastage are minimal.
- It is flexible with regard to its positioning within a process chain.
- It can produce patterned thin films - a key requirement for organic electronics. It should be mentioned however, that manufacturing of highly complex integrated circuits (ICs) has exclusively been performed by specialized techniques deviating from standard inkjet to meet the requirements for a high spatial resolution for ultra-short transistor channel lengths.[7a]

Finally, it is possible to add functionalities using inkjet printing on a substrate that already has electronic structures and devices, fabricated using any other technology. Its non-contact, mask-less and master-less nature, along with the freedom to position the printhead directly on top of any 3D coordinate of the substrate, enable this aspect.

Classification

The inkjet technology is broadly classified into two categories, based on the mechanism of droplet generation.[6] They are *continuous inkjet (CIJ)* and *drop-on-demand inkjet (DOD)*. DOD printing is, in turn, classified into three types, namely *thermal inkjet, piezo inkjet* and *electrostatic inkjet*. **Figure 2** depicts the overall classification of the inkjet printing technology, and the salient features of each individual technology.

In spite of the very high droplet generation frequencies (20-60 kHz), CIJ printing is not widely used in printed electronics as the recycling process after exposure to the environment might result in contamination of the ink. Moreover, CIJ is a potentially wasteful process, as a result of continuous generation of droplets irrespective of presence or absence of information at each pixel of the image or the text to be reproduced. However, CIJ has its advantage when it comes to work on substrates with a non-planar geometry.

As far as the DOD inkjet technologies are concerned, thermal inkjet and electrostatic inkjet lag far behind the piezo inkjet,[8] mainly due to the following reasons:

- Thermal inkjet can lead to degradation of functional materials present in the ink due to the cyclic thermal loading. Piezo inkjet, on the other hand, is an isothermal process. Nontheless, thermal inkjet has successfully proven suitable for the manufacturing of light-emitting diodes based on inorganic quantum dots.[7b]
- The range of ink solvents that could be used in piezo inkjet is much broader than thermal and electrostatic inkjet.
- The investment and running costs needed for an electrostatic inkjet is much higher than piezo inkjet. Moreover, this technique is still under development, and is not as mature as either piezo or thermal inkjet in its evolution.

1. Continuous Inkjet
- Ink column under pressure
- A stream of ink droplets continuously ejected by a nozzle
- Charged droplets deflected and positioned using electric field
- Remaining droplets collected by a gutter and recycled

2. Drop-on-Demand Inkjet
- Droplets ejected on demand, e.g., when an image pixel is ON
- Simpler system than continuous inkjet
- Multiple actuation mechanisms, listed below

2a. Thermal
- Flash heating of the ink by heating element
- Bubble formation resulting in ejection of ink droplet from nozzle

2b. Piezo
- Voltage pulse applied to a piezoelectric transducer (PZT)
- Acoustic wave propagation in ink channel due to PZT actuation
- Ink jet droplet ejection from nozzle

2c. Electrostatic
- Electric field exists between inkjet setup and substrate
- Droplet formation involves complex interaction of surface tension ratio between ink and nozzle, and electric field
- Signal fed to printhead balances forces to create ink droplet

Figure 2. Classification of the most common inkjet printing technologies.[1,8]

Piezo Inkjet

A piezo inkjet system, as its name indicates, consists of a piezoelectric transducer (PZT) that is actuated by a voltage pulse. This is called the *inverse piezoelectric effect*. In commercial printing systems, the frequency of the voltage pulse usually ranges from 1 kHz to 20 kHz. As a result of the piezo actuation, pressure (acoustic) waves are generated and propagated within the ink channel, and droplets are generated at acoustic frequencies.[6]

Figure 3a illustrates the commonly used bipolar waveform,[9a] along with a brief description of the significance of each segment of the waveform. This is just an example - many different types of waveforms can usually be applied to an inkjet printhead to create droplets. The profile and magnitude of the applied waveform depend on the nozzle dimensions, the rheology of the ink used, and the droplet size and velocity desired. **Figure 3b** shows a sequence of pictures depicting the formation of a droplet from a piezo inkjet nozzle.
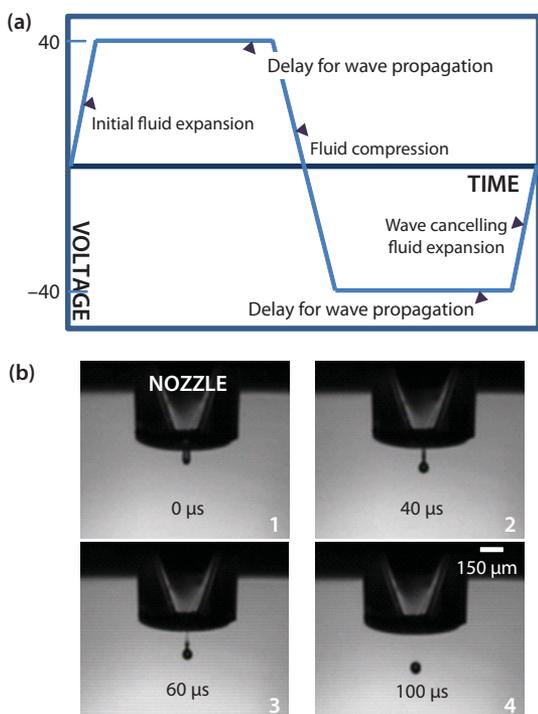
Figure 3. a) Exemplary bipolar waveform for piezo actuation; b) Droplet formation sequence from the nozzle of a piezo inkjet printhead.

Requirements of Inkjet Printing

While the different types of inkjet printing technologies mentioned earlier more or less have similar requirements with respect to materials, pre-processing of the substrates and post-processing of the printed structures, this section focuses especially on the requirements of the piezo inkjet.

Substrate: As mentioned earlier, inkjet printing itself does not depend on the substrate. It is possible to use any type of substrate e.g., rigid, flexible, reinforced and non-reinforced. However, the interaction of the printed ink and the substrate plays a decisive role in determining the accuracy and robustness of the printed structure, and ink properties and substrate properties have to be well matched. As a result, the substrate surface is usually processed prior to printing in order to improve wetting, adhesion, etc. Plasma treatment and corona treatment are widely used for this purpose. For high-definition structures, substrate patterning, i.e., partitioning the substrate surface into hydrophilic and hydrophobic areas, is used.[9b]

Inks: The inks used for printed electronics are either dispersed (pigment-like) or dissolved (dye-like) in one or more solvents.[10] The role of the solvents is to provide a vehicle by means of which functional materials could be carried through the printhead and ejected via the nozzle. In the context of printed electronics, a functional material fulfills an electronic/electrical functionality, e.g., conductivity, semiconductivity, resistivity and dielectricity. Many types of inks that fulfill these functionalities are commercially available.

The key characteristics of a piezo inkjet ink are: dynamic viscosity of less than 20 mPa.s,[11a] surface tension value below 80 mN.m^{-1},[11b] stability of the ink in solution/suspension in the printhead, and the particle size of the ink constituents preferably well below (by orders of magnitude) the nozzle orifice.[11c] These values are just guidelines and the particular values may vary from system to system. The particle loading is also a key factor in determining the stability of the printing process.

Sintering/Curing: Unlike graphical printing, where the functionality light absorption (hence: color) is more or less achieved immediately after the deposition process and drying of the layer, usage of functional inks "beyond color" requires a suitable transformation of the deposited ink layer to render it functional. This is done to remove the solvents and other additives such as surfactants, dispersants, humectants, adhesion enhancers, etc., which are present in the ink. In the case of (pigment-like) metal nanoparticle inks, for instance, the printed structure has to be sintered, so that the nanoparticles can join together and form a continuous percolating structure that allows for conductivity. For (dye-like) metal-organic decomposition (MOD) inks, the molecular complexes have to be broken up to enable formation of metal clusters. In both cases, sintering is then usually accomplished by the application of heat. To render the technique suitable for flexible plastic substrates that are thermally instable, other sintering techniques such as continuous,[12a] flash UV radiation,[12b] plasma treatment,[12c] or laser-assisted sintering,[12d] microwave-assisted sintering,[12e] DC or AC electric fields[12f,12g] or chemical sintering[12h] have been proposed. The sintering sequence of a metal nanoparticle ink due to the application of heat is depicted in **Figure 4**.

A: Nanoparticles dispersed in solvent
B: Solvent evaporation due to heating
C: Evaporation of other additives
D: Sintering of nanopartaicles/increase in grain size
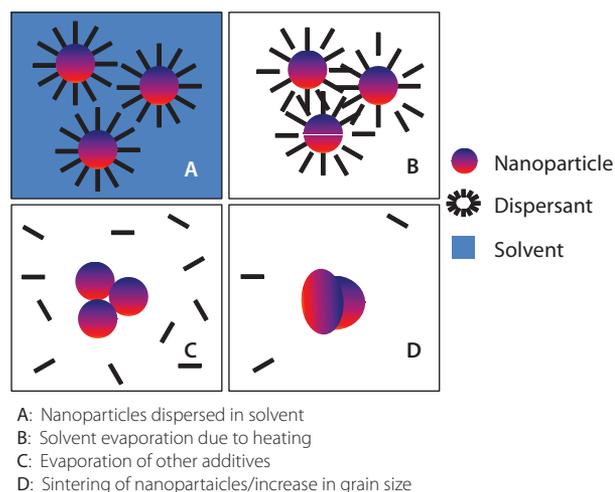
Figure 4. Sintering sequence of a metal nanoparticle based ink.[13]

The quality of sintering is an important issue. Due to the presence of residues, the printed structures are almost always less than 100% dense, even after sintering. Moreover, thermal sintering is not suitable for all types of substrates, as the sintering temperature is usually larger than 150 °C - many polymer substrates cannot withstand such temperatures. In the case of organic polymer inks, the printed structure is cured rather than sintered. Curing refers to the hardening of polymers due to cross-linking.

Application Examples

There are numerous application examples that demonstrate the suitability of inkjet printing for printed electronics; only a selected few are presented here.
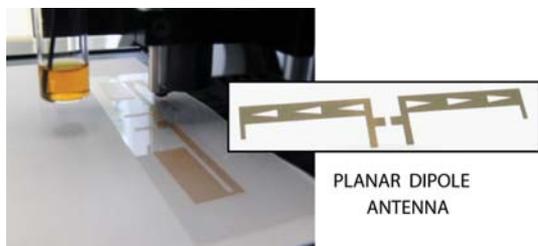
Figure 5. Inkjet printing of a planar dipole antenna with a resonance frequency of 868 MHz, using silver ink, at TU Chemnitz/Fraunhofer ENAS, Germany.[14]

Figure 5 shows one such application: an inkjet-printed planar dipole antenna for ultra-high frequency (UHF) range, on flexible and rigid substrates.[14] Filter, transmission line, and patch antenna for the same frequency range have also been inkjet-printed and reported.[8,15]

Inkjet printing has been successfully used to fabricate passive electrical components. It has also surpassed spin coating as an effective manufacturing method to fabricate organic or polymer light emitting devices (OLED/PLED). In fact, high-resolution patterning of an all-polymer thin-film transistor (TFT) using inkjet printing has already been achieved. However, these devices are currently restricted to low-end applications e.g., radio frequency identification tags (RFID), as the active materials they are made of have low mobility. Moreover, their switching speeds are low.[16-17] Another active area of research is solar energy. Inkjet-printed organic solar cells were demonstrated by Konarka Technologies Inc. Research activities are currently underway to inkjet print high-efficiency solar cells using inorganic materials.[17]

Conclusions and Outlook

Inkjet printing holds a lot of promise to revolutionize the way electronics are manufactured. Even though there are not many products in the market that are fully inkjet-printed, efforts are well underway to surmount the challenges.

One of the most important factors that would play a decisive role in the success of inkjet printing in electronics applications is the advancement in materials development, that is, ink development. Inks containing functional materials that offer high performance such as high mobility,

at lower sintering temperatures, besides reliably high printability will enable inkjet printing of high performance electronic devices on a variety of substrate materials. The success of inkjet printing might also depend on how quickly the alternative sintering and curing techniques mature, so that heat addition to the printed flexible substrate can be kept minimal. Finally, the resolution of inkjet printing, which is much lower than photolithography, will be a limiting factor in its application in high density circuit fabrication.

References

(1) Kipphan, H. Ed.; Handbook of Print Media; Springer, Germany, **2001**.
(2) Océ Digital Printing; Océ Printing Systems GmbH, Germany, 10th ed., **2006**.
(3) Printed Electronics: A Manufacturing Technology Analysis and Capability Forecast; NanoMarkets report: www.nanomarkets.net, **2007**.
(4) Parashkhov, R.; Becker, E.; Riedl, T.; Johannes, H.-H.; Kowalsky, W. *Proc. IEEE* **2005**, *93*, 7.
(5) Vornbrock, A. D. L. F.; Sung, D.; Kang, H.; Kitsomboonloha, R.; Subramanian, V. *Org. Electron.* **2010**, *11*, 2037.
(6) Derby, B. *Annu. Rev. Mater. Res.* **2010**, *40*, 395.
(7) a) Sekitani, T.; Noguchi, Y.; Zschieschang, U.; Klauk, H.; Someya, T. *Proc. Nat. Acad. Sci.* **2008**, *105* (13), 4976; b) Wood, V.; Panzer, M. J.; Chen, J. L.; Bradley, M. S.; Halpert, J. E.; Bawendi, M. C.; Bulovic, V. *Adv. Mater.* **2009**, *21* (21), 2151.
(8) Sridhar, A. An Inkjet Printing-Based Process Chain for Conductive Structures on Printed Circuit Board Materials. Ph.D. Thesis, University of Twente, the Netherlands, 2010.
(9) a) Herlogsson, L.; Noh, Y. Y.; Zhao, N.; Crispin, X.; Sirringhaus, H.; Berggren, M. *Adv. Mater.* **2008**, *20* (24), 4708; b) Lim, J. A.; Lee, W. H.; Kwak, D.; Cho, K. *Langmuir* **2009**, *25* (9), 5404. c) Wallace, D. B.; Shah, V.; Hayes, D. J.; Grove, M. E. *J. Imaging Sci. Technol.* **1996**, *40*, 5.
(10) Kamyshny, A.; Ben-Moshe, M.; Aviezer, S.; Magdassi, S. *Macromol. Rapid Commun.* **2005**, *26*, 281–288.
(11) a) de Gans, B.-J.; Duineveld, P. C.; Schubert, U. S. *Adv. Mater.* **2004**, *16*, 3; b) de Gans, B. J.; Kazancioglu, E.; Meyer, W.; Schubert, U. S. *Macromol. Rapid Commun.* **2004**, *25*, 292; c) Shin, D. Y.; Smith, P. J. *J. Appl. Phys.* **2008**, *103* (11), 114905.
(12) a) Jahn, S. F.; Blaudeck, T.; Baumann, R. R.; Jakob, A.; Ecorchard, P.; Rüffer, T.; Lang H.; Schmidt, P. *Chem. Mater.* **2010**, *22*, 10; b) Yung K. C.; Gu, X.; Lee, C. P.; Choy, H. S.; *J. Mater. Proc. Tech.* **2010**, *210* (15), 2268; c) Reinhold I.; Hendriks, C. E.; Eckardt, R.; Kranenburg, J. M.; Perelaer, J.; Baumann, R. R.; Schubert, U. S. *J. Mater. Chem.* **2009** *19* (21) 3384; d) Yung, K. C.; Plura, T. S.; *Appl. Phys. A: Mater. Sci. Proc.* **2010**, *101*, 393; e) Perelaer J.; de Gans, B. J.; Schubert, U. S. *Adv. Mater.* **2006**, *18* (16), 2101; f) Allen M. L.; Aroniemi M.; Mattila, T.; Alastalo, A.; Ojanpera, K.; Suhonen, M.; Seppä, H. *Nanotechnology* **2008**, *19* (17), 175201; g) Allen M. L.; Leppäniemi, J.; Vilkman, M.; Alastalo, A.; Mattila, T. *Nanotechnology* **2010**, *21* (47), 475204; h) Valeton, J. J. P.; Hermans, K; Bastiaansen, C. W. M.; Broer, D. J.; Perelaer, J.; Schubert, U. S.; Crawford, G. P.; Smith, P. J. *J. Mater. Chem.* **2010**, *20* (3), 543.
(13) Harima Silver Nanopaste (NPS-J) Datasheet; Harima Chemicals Inc., Japan.
(14) Zichner, R.; Siegel, F.; Hösel, M.; Baumann, R. R. *Proceedings of the LOPE-C* **2010**, pp. 13-16.
(15) Mantysalo, M.; Mansikkamaki, P. *AEU Int. J. Electron. Commun.* **2009**, *63*, 1.
(16) Ben-Tzvi, P.; Rone, W. *Microsyst. Technol.* **2010**, *16*, 3.
(17) Singh, M.; Haverinen, H. M.; Dhagat, P.; Jabbour, G. E. *Adv. Mater.* **2010**, *22*, 6.

For questions, product data, or new product suggestions, please contact Aldrich Materials Science at *matsci@sial.com*.

ALDRICH® Materials Science

15

Inks for Printing Applications

For a complete list of available products, please visit *aldrich.com/printedelectronics*

Name	Structure	Concentration	Resistivity	Form	Prod. No.
Silver nanoparticle ink, SunTronic® Silver*	Ag	in ethanol and ethanediol 20 wt. % (dispersion in organic solvents)	volume resistivity 5-30 µΩ-cm (after annealing @ 150-300 °C)	-	719048-5ML 719048-25ML
Silver nanoparticle ink, Silverjet DGP-40LT-15C**		30-35 wt. % in triethylene glycol monomethyl ether	11 µΩ-cm surface tension 35-38 dynes/cm	dispersion	736465-25G 736465-100G
Silver nanoparticle ink, Silverjet DGP-40TE-20C**		30-35 wt. % in triethylene glycol monomethyl ether	~7 µΩ-cm surface tension 35-38 dynes/cm	dispersion	736473-25G 736473-100G
Silver nanoparticle ink, Silverjet DGP-45HTG**		30-35 wt. % in triethylene glycol monomethyl ether	~2 µΩ-cm surface tension 35-38 dynes/cm	dispersion	736481-25G 736481-100G
Silver nanoparticle ink, Silverjet DGH-55LT-25C**		50-60 wt. % in tetradecane	27-30 dynes/cm ~2.7 µΩ-cm	dispersion	736503-25G 736503-100G
Silver nanoparticle ink, Silverjet DGH-55HTG**		50-60 wt. % in tetradecane	~2.2 µΩ-cm surface tension 27-30 dynes/cm	dispersion	736511-25G 736511-100G
Silver, Silver Paste DGP80 TESM8020**		70-80% solid content in α-Terpineol	1-3 µΩ-cm	paste (microparticles)	735825-25G

*Product of Sun Chemicals
**Product of ANP, Inc.
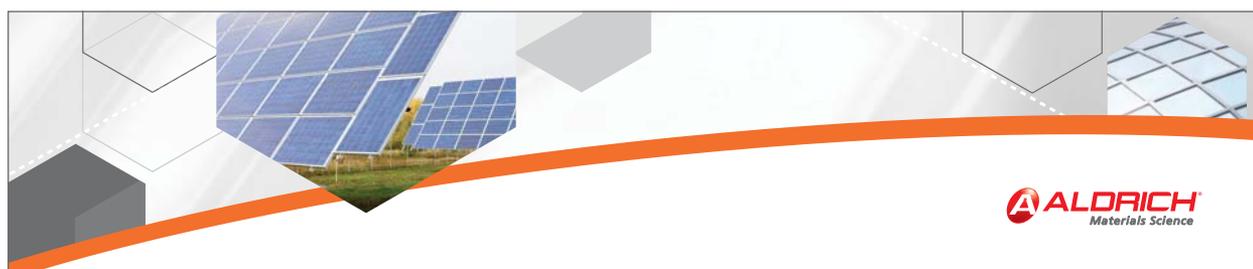
Aldrich® Materials Science Presents Ready-to-Use Ink Systems!

Plexcore® PV Ink System (Aldrich Prod. No. 711349)

- Plexcore PV 1000 photoactive ink
  Application: Semiconducting ink (PCBM/P3HT Mixture) for Photoactive Layers
- Plexcore PV 1000 hole transport ink
  Application: Conductive ink (sulfonated polythiophene) for hole transport layers

Organic photovoltaic cell structure
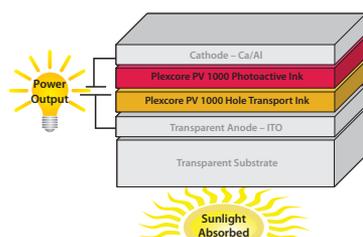
Plexcore® OC Ink Kit (Aldrich Prod. No. 719102)

- Selection of organic conductive inks with varying resistivities and work functions for highly tunable hole injection layers (HILs)

OLED device stack
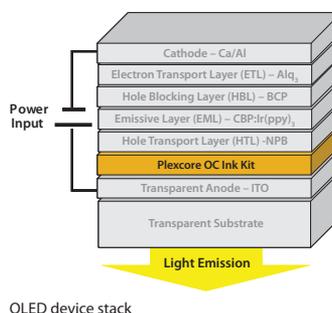
For detailed product and application information, please view our technology spotlights at *aldrich.com/oel*

Plexcore is a registered trademark of Plextronics, Inc.

sigma-aldrich.com

SIGMA-ALDRICH®

Substrates for Printing Applications

For a complete list of available products, please visit *aldrich.com/printedelectronics*

Plastic Substrates

Name	Structure	Dimensions	Surface Resistivity (Ω/sq)	Prod. No.
Indium oxide coated PET, IO-PET	In_2O_3	slide, L × W × D 150 × 150 × 0.2 mm	≤10	700177-5PAK 700177-10PAK
Indium oxide coated PET, IO-PET		slide, L × W × D 150 × 150 × 0.2 mm	60-100	702811-5PAK 702811-10PAK
Indium tin oxide coated PET, ITO-PET	In_2O_3 / SnO_2	sheet, L × W × D 1 ft × 1 ft × 5 mil	60	639303-1EA 639303-5EA
Indium tin oxide coated PET, ITO-PET		sheet, L × W × D 1 ft × 1 ft × 5 mil	100	639281-1EA 639281-5EA

Glass Substrates

Name	Structure	Dimensions	Surface Resistivity (Ω/sq)	Prod. No.
Indium tin oxide coated glass slide, rectangular, ITO	In_2O_3 / SnO_2	slide, L × W × D 75 × 25 × 1.1 mm	8-12	578274-10PAK 578274-25PAK
Indium tin oxide coated glass slide, rectangular, ITO		slide, L × W × D 75 × 25 × 1.1 mm	15-25	636916-10PAK 636916-25PAK
Indium tin oxide coated glass slide, rectangular, ITO		slide, L × W × D 75 × 25 × 1.1 mm	30-60	636908-10PAK 636908-25PAK
Indium tin oxide coated glass slide, rectangular, ITO		slide, L × W × D 75 × 25 × 1.1 mm	70-100	576352-10PAK 576352-25PAK
Indium tin oxide coated glass slide, square, ITO		slide, L × W × D 25 × 25 × 1.1 mm	8-12	703192-10PAK
Indium tin oxide coated glass slide, square, ITO		slide, L × W × D 25 × 25 × 1.1 mm	70-100	703176-10PAK
Indium tin oxide coated glass slide, square, ITO		slide, L × W × D 25 × 25 × 1.1 mm	30-60	703184-10PAK
Fluorine doped tin oxide coated glass slide, FTO, TEC 7	F/SnO_2	50 × 50 mm	~7	735140-5EA
		100 × 100 mm	~7	735159-5EA
		300 × 300 mm	~7	735167-1EA
Fluorine doped tin oxide coated glass slide, FTO, TEC 8		50 × 50 mm	~8	735175-5EA
		100 × 100 mm	~8	735183-5EA
		300 × 300 mm	~8	735191-1EA
Fluorine doped tin oxide coated glass slide, FTO, TEC 10		50 × 50 mm	~10	735205-5EA
		100 × 100 mm	~10	735213-5EA
		300 × 300 mm	~10	735221-1EA
Fluorine doped tin oxide coated glass slide, FTO, TEC 15		50 × 50 mm	~15	735248-5EA
		100 × 100 mm	~15	735256-5EA
		300 × 300 mm	~15	735264-1EA

For questions, product data, or new product suggestions, please contact Aldrich Materials Science at *matsci@sial.com*.

ALDRICH® Materials Science

17

Conductive Polymers for Advanced Micro- and Nano-fabrication Processes

Rafal Dylewicz[1], Norbert Klauke[2], Jon Cooper[2] and Faiz Rahman[1]*
[1] Optoelectronics Research Group, School of Engineering, University of Glasgow, Rankine Building, Oakfield Avenue, Glasgow G12 8LT, United Kingdom
[2] Bioelectronics Research Centre, School of Engineering, University of Glasgow, United Kingdom
*Email: Faiz.Rahman@glasgow.ac.uk

Introduction

Conducting polymers such as polyaniline, polythiophene and poly-fluorenes are now much in the spotlight for their applications in organic electronics and optoelectronics. Such materials are used, for example, in making organic thin-film transistors and light-emitting diodes. Here, we present a novel application of conductive polymer thin films – for use as charge dissipation layers for *state-of-the-art* patterning techniques, i.e., electron-beam lithography (EBL) and focused ion beam (FIB) etching, on demanding substrates. The ability of thin polythiophene layers to dissipate accumulated charge in electron-beam lithography of wide bandgap semiconductors, e.g., zinc oxide[1] and gallium nitride[2], as well as for focused ion beam patterning of glass is demonstrated here. The former technique (EBL) is related to the creation of dense periodic nanopatterns in hydrogen silsesquioxane (HSQ) negative-type e-beam resist, so that passive photonic devices could be fabricated in a semiconductor by a subsequent dry etch process. The latter technology (FIB etching) is related to biomedical applications as glass capillaries are routinely used in electrophysiological investigations of mammalian cells.[3]

In each case, we used commercially-available 2.5% aqueous dispersion of poly(3,4-ethylenedioxythiophene)-poly(styrenesulfonate) from Sigma-Aldrich (PEDOT:PSS, Aldrich Prod. No. 655201). The high electrical conductivity and good oxidation resistance of these polymer films make them suitable for electromagnetic shielding and noise suppression applications. The optical transmission spectrum of the polythiophene film deposited on a float glass substrate revealed a featureless transmission curve.[2] Thus, the polymer film was found to possess high transparency throughout the visible light spectrum and even into near IR and near UV regions. In addition, values of extinction coefficient *k* for a thin polythiophene film are negligible in a wide range of wavelengths, including the visible light spectrum, as experimentally determined with the use of a rotating analyzer ellipsometer. The optical transparency of polythiophene charge dissipation layers makes it easy to see the sample surface and perform any alignment operations required to align patterns with pre-existing device features.

Sample Processing Using PEDOT:PSS Conductive Polymer

Conductive Polymers for Electron-beam Lithography (EBL)

A quick and inexpensive processing method has been developed for EBL exposure of dense and high-resolution patterns in hydrogen silsesquioxane (HSQ) negative-type resist deposited on bulk ZnO and on GaN/AlN-on-sapphire substrate. Zinc oxide (ZnO, Aldrich Prod. No. 255750) is a wide bandgap semiconductor that is attracting much attention these days owing to its potential for fabricating blue light emitting devices, thin-film transistors (TFTs) and potentially even laser diodes. This II-VI oxide semiconductor has about the same bandgap (~3.4 eV) as gallium nitride (GaN, Aldrich Prod. No. 481769) which is now the standard material for making short wavelength light emitting diodes and laser diodes. ZnO, however, is not just an alternative material but has a number of advantages over GaN when it comes to making similar devices. These include a higher exciton binding energy and the availability of bulk substrates. III-V-Nitride compounds (GaN, InN and AlN) are interesting and prospective materials for future optoelectronics applications. These new materials can be indispensable in violet and UV spectral regions, but they are also very useful for the generation and detection of blue and green light. All III-V nitrides have a direct energy band-gap, a valuable feature which increases their usefulness over indirect band-gap semiconductors for making both light emitters and light detectors. There is also the possibility of forming solid solutions with InN (Aldrich Prod. No. 490628) and AlN (Aldrich Prod. No. 241903), which allows tailoring optical and electrical properties. GaN also exhibits high mechanical and thermal stability, which makes it very useful for high-temperature electronic and optoelectronic applications such as power transistors, high power LEDs and lasers.

Both electron microscope inspection and electron-beam lithography patterning of ZnO and GaN face difficulties because these materials are not able to efficiently dissipate the charge that accumulates during such processes. Consequently, e-beam lithography of wide bandgap semi-conductors is commonly performed with a thin conducting metal layer, usually aluminum, deposited on top of the e-beam resist. Furthermore, the processing of ZnO is difficult since it is an amphoteric oxide, which is easily attacked by both acids and bases, e.g., used for the removal of metal films. Here, we describe a much simpler technique, in comparison with metal layer evaporation. It can be widely used without any special resist preparation steps. The use of commercially available PEDOT:PSS conductive polymer to dissipate charge in electron-beam lithography is schematically presented in **Figure 1**, using an epitaxial GaN/AlN/sapphire sample. Processing involves spin-coating of a conductive polymer (PEDOT:PSS) on top of a HSQ-coated sample, electron-beam writing of dense patterns in resist, removal of the PEDOT:PSS layer and, finally, development of the exposed HSQ e-beam resist. Comparison of experimental results is given here for two different cases, where no charge dissipation layer was used, as well as the case where a 100-nm-thick conductive polymer layer was deposited on top of the HSQ resist (**Figure 2**). Scanning-electron microscope (SEM) observations of the resulting photonic crystal (PhC) patterns, exposed with the same dose of 442 $\mu C/cm^2$, are shown in **Figure 2**, at two different magnifications 2k and 70k. The fabricated nano-patterns included a 50 $\mu m \times 10 \mu m$ area of pattern W1 (one row of holes removed) and W3 (three rows of holes removed) photonic crystal waveguide structures with a triangular lattice of holes (periodicity of 550 nm, designed hole diameter of 440 nm). For the pure HSQ case (**Figure 2a**) severe overexposure of the periodic pattern was observed. Despite properly

defined holes on the edges of an array, the middle part of the PhC lattice exhibited signs of strong proximity effect, which is indicated by a decrease in SEM observation contrast. In the case where the conductive polymer was used, however, sharply defined holes were obtained within highly uniform photonic crystal lattices, as additionally indicated by high contrast SEM micrographs (**Figure 2b**).

(a) Spin-coating of PSS:PEDOT

(b) Electron-beam Lithography

PSS: PEDOT conductive polymer (100 nm)

HSQ e-beam resist (670 nm)

GaN (500 nm)

AlN (100 nm)

Sapphire substrate

(d) HSQ Resist Development

⌀ 359 nm

(c) Removal of PSS:PEDOT
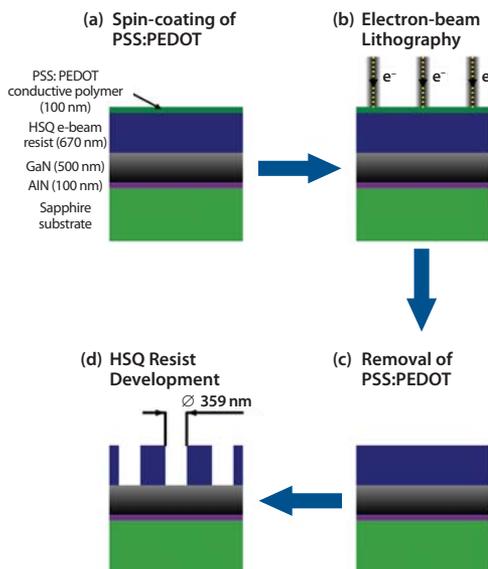
Figure 1. Schematic presentation of the experimental HSQ/PEDOT:PSS/GaN/AlN/Al$_2$O$_3$ sample patterned by electron-beam lithography with the use of a conductive polymer charge dissipation layer: **a)** deposition of thin PEDOT:PSS film by a spin-coating technique; **b)** writing a pattern in HSQ resist with electron-beam-based process; **c)** removal of PEDOT:PSS in warm bath of deionised water; **d)** development of HSQ resist, dense nano-patterns are revealed in the resist layer.

After processing, spin-coatable conducting polymer may be easily removed due to its solubility in water, which makes it a perfect solution for the processing of amphoteric oxide samples, e.g., zinc oxide. Gallium nitride processing also benefits from polymer dissipation layer usage due to extended exposure range and the avoidance of dense pattern overexposure in HSQ. The new approach provides the ability to make ZnO and GaN sample processing much simpler, quicker, and less expensive, but it may also be extended to EBL exposures of many other semiconductor/dielectric materials, as described in the next paragraph.

(a)

(b)
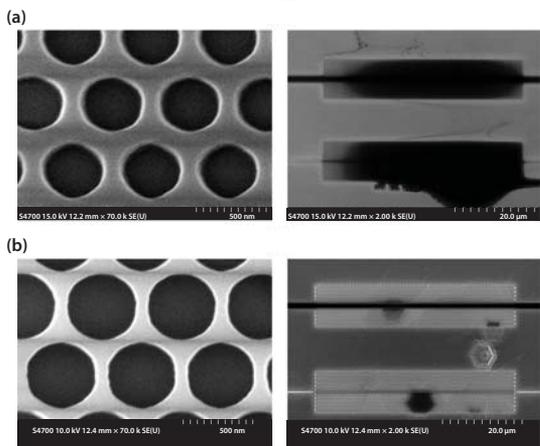
Figure 2. Scanning-electron microscope (SEM) pictures (top-view) of a photonic crystal lattice in HSQ resist on bulk ZnO sample, for an e-beam exposure dose of 442 μC/cm^2: **a)** e-beam exposure process without a conductive polymer used; **b)** e-beam exposure process with thin conductive polymer used.

Conductive Polymers for Focused Ion Beam (FIB) Etching

A water-soluble film formed by a PEDOT:PSS conductive polymer was also used to prevent electrical charging during ion milling of a glass material. Ion milling is performed using a tightly focused beam of ions to ablate material with nanometer precision. This is achieved as the beam positioning and the milling progress are both monitored *in-situ* with a scanning-electron microscope. In our experiments, glass capillaries were used as the target material to be patterned on micro-scale. Glass capillaries are commonly used in electrophysiological investigations of mammalian cells (e.g., microelectrodes for patch clamp), where the locally heated capillaries are pulled to form a tapered tip with an opening ranging from 1 μm to 100 μm in diameter. The tapered tip of a pulled capillary is routinely used for locally altering the concentration of a substance in solution in a spatially and temporarily defined manner.[3] Glass capillaries can be pulled to form hollow filaments (~30 μm inner diameter) with thin walls (~5 to 10 μm thick). Perforation of these filaments at defined locations would enable the formation of two compartments (inside/outside of the capillary), communicating only through the openings in the capillary wall. With one end of the liquid-filled capillary pressurized and the other end closed one could use this arrangement to apply the liquid to predefined locations. This is because the openings in the capillary wall allow the liquid to leave the inside of the capillary and diffuse into the solution outside. To fabricate well-defined openings in a capillary wall a FIB patterning was used. A prerequisite of FIB processing is a conductive coating e.g., with a *AuPd* metal layer sputter-coated in an inert argon gas atmosphere. This is to stop the charging of the glass material and thus avoid the drifting of the ion beam. Ideally, one wants to remove the conducting film after the milling process in order to regain the transparency of the glass; for further optical investigations (light microscopy). Previously the capillaries were sputter-coated with thin *AuPd* layer, and the metal film was removed after the milling process by soaking in a jar filled with HCN + KOH vapour.[4] This technique involves the handling of the highly toxic KCN powder and the generation of HCN gas. Because of the extensive precautions required during this process, an alternative to sputter-coating is desirable. Again, a conductive organic polymer film provides the best solution. In the present case, the PEDOT:PSS film was deposited on the glass surface through a simple dip-coating technique, i.e., the capillary was placed into a container with the aqueous PEDOT:PSS dispersion and slowly withdrawn, leaving a thin coat of the polymer on its surface. After the FIB milling process the polymer film was easily removed by soaking the capillary in water. The smallest diameter of 5 μm as seen in **Figures 3a** and **3b**, respectively.

a) ⌀ ~5 μm

b) 20 μm

Through-holes etched by FIB

Flow of 1-μm-diameter fluorescence beads

20 μm
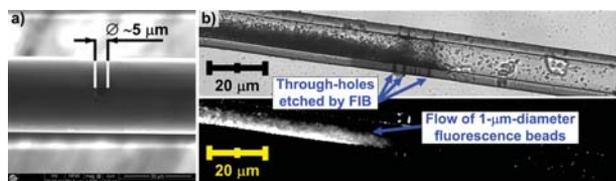
Figure 3. Experimental results of focused ion beam pattering of glass capillaires: **a)** scanning-electron microscope picture of an opening in a capillary wall, processed with the use of PEDOT:PSS layer; **b)** transmission (top) and fluorescence (bottom) con-focal light microscopy image of the fabricated glass capillary. Please note three through-holes indicated in the lower wall of the glass capillary. The flow of fluorescence beads (small particles with diameter of ~1 μm) from the outside to the inside of the capillary, through the milled holes, is indicated by the presence of densely packed beads on the inside downstream of the through-holes.

For questions, product data, or new product suggestions, please contact Aldrich Materials Science at *matsci@sial.com*.

ALDRICH® Materials Science

19

Conclusions

The excellent performance of PEDOT:PSS conductive polymer to dissipate charge in both electron-beam lithography and focused ion beam milling has been demonstrated experimentally. Using the PEDOT:PSS dissipation layer provides the ability to make sample processing simpler, quicker and less expensive for a variety of substrates, including gallium nitride (GaN) on sapphire (Al_2O_3) substrates, zinc oxide (ZnO), fused silica, lithium niobate ($LiNbO_3$), silicon carbide (SiC) and diamond (C).

Acknowledgments

References

(1)   Dylewicz, R.; Lis, S.; De La Rue, R. M.; Rahman, F. *Electron. Lett.* **2010**, *46*, *1025*.
(2)   Dylewicz, R.; Lis, S.; De La Rue, R. M.; Rahman, F. *J. Vac. Sci. Technol. B* **2010**, *28*, *817*.
(3)   Klauke, N.; Smith, G. L.; Cooper, J. M. *Anal. Chem.* **2007**, *79*, *1205*.
(4)   Leslie S. A; Mitchell J. C. *Palaeontology* **2007**, *50*, *1459*.

Conductive Polymers

For a complete list of available products, please visit *aldrich.com/conductingpoly*

PEDOT Polymers

Name	Conductivity	Composition	Properties	Prod. No.
Poly(3,4-ethylenedioxythiophene)-poly (styrenesulfonate), PEDOT:PSS	1 S/cm	PEDOT content 0.5 wt. % PSS content 0.8 wt. %	1.3 wt % dispersion in H_2O	483095-250G
	150 S/cm (18 μm film thickness)	-	2.2-2.6% in H_2O	655201-5G 655201-25G
	~ 1E-5 S/cm	PEDOT content ~ 0.14% PSS content ~ 2.6%	2.8 wt % dispersion in H_2O	560596-25G 560596-100G
Poly(3,4-ethylenedioxythiophene), tetramethacrylate end-capped solution, PEDOT*	0.1-0.5 S/cm (bulk conductivity)	*p*-toluenesulfonate as dopant, Oligotron™ tetramethacrylate 0.5 wt. % propylene carbonate 99.5 wt. %	average M_n ~6,000 ~1,360-1,600 g/mol (methacrylate equivalent weight), 0.5 wt. % (dispersion in propylene carbonate)	649813-25G
	0.1-0.5 S/cm (bulk conductivity)	*p*-toluenesulfonate as dopant, Oligotron™ tetramethacrylate 0.5 wt. % ethanol 5.8 wt. % isopropanol 0.3 wt. % nitromethane 93.4 wt. %	average M_n ~6,000 ~1,360-1,600 g/mol (methacrylate equivalent weight), 0.5 wt. % (dispersion in nitromethane)	649821-25G
Poly(3,4-ethylenedioxythiophene), bis-poly(ethyleneglycol), lauryl terminated, PEDOT:PEG*	0.010-0.0010 S/cm (bulk)	*p*-toluenesulfonate as dopant, Aedotron™ TM-P3 polymer 0.8-1.2 wt. % ethanol 4-8 wt. % isopropanol 0.2-0.8 wt. % nitromethane 90-95 wt. %	0.7 wt. % (dispersion in nitromethane) 0.5-0.9 wt. % (solid concentration)	736295-25G
	0.01-0.05 S/cm (bulk)	*p*-toluenesulfonate as dopant, 1,2-Dichloro-benzene 90-95 wt. % Aedotron™ TM-P3 polymer 0.3-0.8 wt. % ethanol 4-8 wt. % isopropanol 0.2-0.8 wt. % processing additive 0.1-0.4 wt. %	0.6-1.0 wt. % (solid) 0.7 wt. % (dispersion in 1,2-dichlorobenzene)	736309-25G
	10-45 S/cm (bulk)	perchlorate as dopant, Aedotron™ TM-C3 polymer 0.2-0.9 wt. % acetonitrile 4-8 wt. % propietary processing additive 0.1-0.7 wt. % propylene carbonate 90-95 wt. % propylene glycol 0.0-0.3 wt. %	0.6-1.1 wt. % 0.8 wt. % (dispersion in propylene carbonate)	736287-25G
	10-60 S/cm	Acetonitrile 4-8 wt. % Aedotron™- C3 polymer 0.2-0.7 wt. % Nitromethane 90-95 wt. % Propylene glycol 0.0-0.3 wt. % proprietary processing additive 0.1-0.7 wt. %	0.4-0.9 wt. % (content of dispersion)	687316-25G
Poly(3,4-ethylenedioxythiophene)-*block*-poly(ethylene glycol) solution, PEDOT:PEG	0.5-3 S/cm (bulk)	perchlorate as dopant	1 wt % dispersion in nitromethane	649805-25G
Polypyrrole-*block*-poly(caprolactone), PPy-*block*-PCL*	10-40 S/cm (bulk)	*p*-toluenesulfonate as dopant, Biotron™ PP polymer 0.3-0.7 wt. % ethanol 4-8 wt. % nitromethane 90-95 wt. %	0.3-0.7 wt. % (dispersion in nitromethane) 0.3-0.7 wt. % (solid)	735817-25G

*Products of TDA Research, Inc.

Polythiophenes

Name	Structure	Electronic Properties	Form	Prod. No.
Poly(3-octylthiophene-2,5-diyl-co-3-decyloxythiophene-2,5-diyl), POT-co-DOT		-	powder	696897-250MG
Poly(thiophene-3-[2-(2-methoxyethoxy)ethoxy]-2,5-diyl), sulfonated solution, Plexcore®OC RG-1200*		resistivity 500-3,000 Ω-cm work function −5.1-−5.2 eV	liquid, 2% in ethylene glycol monobutyl ether/water, 3:2	699780-25ML
Poly(thiophene-3-[2-(2-methoxyethoxy)ethoxy]-2,5-diyl), sulfonated solution*		resistivity 25-250 Ω-cm work function −5.1-−5.2 eV	liquid, 2% in 1,2-propane-diol/isopropanol/water, 3:2:1	699799-25ML
Poly(3-octylthiophene-2,5-diyl), regioregular, P3OT		-	solid	682799-250MG
Poly(3-hexylthiophene-2,5-diyl), >98% head-to-tail regioregular (HNMR) regioregular, P3HT*		-	solid	698997-250MG 698997-1G 698997-5G
Poly(3-hexylthiophene-2,5-diyl), >95% head-to-tail regioregular (HNMR) regioregular, P3HT*		-	solid	698989-250MG 698989-1G 698989-5G
Poly(3-dodecylthiophene-2,5-diyl), regioregular, P3DDT		-	solid	682780-250MG

*Product of Plextronics

Polypyrrole

Name	Structure	Conductivity	Form	Prod. No.
Polypyrrole doped, PPy	• X organic acid anion	> 0.0005 S/cm (dried cast film)	5 wt % dispersion in H$_2$O	482552-100ML
Polypyrrole, coated on titanium dioxide doped, PPy		0.5-1.5 S/cm (pressed pellet, typical)	solid	578177-10G
Polypyrrole, PPy		10-40 S/cm	solid	577030-5G 577030-25G
Polypyrrole, composite with carbon black doped, PPy		30 S/cm (bulk)	solid	530573-25G
Polypyrrole, composite with carbon black undoped, PPy		~ 8.5 S/cm	solid	577065-10G

Polyaniline

Name	Structure	Conductivity	Form	Prod. No.
Polyaniline (emeraldine salt), PANI		2-4 S/cm (compacted powder)	powder (Infusible)	428329-5G 428329-25G
Polyaniline (emeraldine salt), composite (30 wt.% polyaniline on nylon),PANI		~ 0.5 S/cm	solid	577073-10G
Polyaniline (emeraldine salt), composite (20 wt.% polyaniline on carbon black), PANI		30 S/cm (bulk, typical)	powder	530565-5G 530565-25G
Polyaniline (emeraldine salt), PANI		10-20 S/cm (film)	liquid, 2-5 wt. % (dispersion in xylene)	650013-10ML 650013-50ML
Polyaniline (emeraldine salt), PANI		~ 1 S/cm (film)	liquid, 0.5 wt. % (dispersion in mixed solvents)	649996-10ML

For questions, product data, or new product suggestions, please contact Aldrich Materials Science at *matsci@sial.com*.

21

ALDRICH® Materials Science

Micro and Nanometer Scale Photopatterning of Self-Assembled Monolayers

Graham J. Leggett*
Department of Chemistry, University of Sheffield, Brook Hill,
Sheffield S3 7HF, United Kingdom
*Email: Graham.Leggett@shef.ac.uk

Introduction

Self-assembled monolayers (SAMs) have attracted enormous interest for a wide variety of applications in micro- and nano-technology. In this article, we compare the benefits of three different classes of SAM systems (alkylthiolates on gold, alkylsilanes on silicon dioxide and alkylphosphonic acids on oxide surfaces), and illustrate how photo-patterning techniques can be used to fabricate structures with sizes from 10 nm upwards over areas ranging from a few microns to square centimeters in size. Self-assembled monolayers[1-3] have become indispensible tools in many areas of nanoscience. A SAM is isostructural with a Langmuir-Blodgett (LB) film – it consists of a close-packed, ordered layer of molecular adsorbates on a solid surface – but unlike an LB film, it is deposited in a simple process involving immersion of a substrate in a dilute solution of the adsorbate. The monolayer assembly process is driven by the formation of a strong specific interaction between the adsorbate and substrate, but intermolecular interactions significantly enhance stability and drive ordering. Although the term "self-assembled monolayer" is often used loosely, to refer to almost any organic adsorbate system, strictly speaking a SAM has the following features: (a) a monolayer of amphiphilic molecules adsorbed on a solid surface; (b) a strong (usually chemisorption) adsorbate-substrate interaction; (c) close-packing; and, usually, (d) a high degree of order.

Alkylthiolate SAMs

SAMs of alkythiolates on gold are formed by immersion of a gold film, formed on a suitable substrate, into a dilute (1 mMol) ethanolic solution of the appropriate adsorbate. They exhibit excellent chemical stability and a high degree of order (in 5–10 nm domains, they are effectively crystalline), because of the strength of the Au–S interaction, the similarity in the spacing between adsorption sites (4.99 Å) and the van der Waals diameter of an alkyl chain (4.5 Å). Alklythiolates also form SAMs on a variety of other metals (Ag, Cu and Pd have been widely studied) and some semiconductors (e.g., GaAs).

The principal limitations on the use of alkylthiolate SAMs arise from their modest thermal and oxidative stability: alkylthiolates desorb from surfaces at temperatures not much higher than room temperature, making many types of solution-phase processing difficult; and they exhibit a high susceptibility to ambient oxidation, most likely due to atmospheric ozone, which attacks the S–Au bond. Often, for example in biology, a low density of defects introduced by partial oxidative degradation may lead to a significant impairment of performance. Finally, the requirement to use a gold substrate is also a limitation. For example, gold has a propensity to quench fluorescence, a problem where optical characterization of adsorbed biomolecules is required.

The most widely used patterning technique for alkylthiolate SAMs is microcontact printing (μCP),[4] originally developed by Whitesides and co-workers as an inexpensive alternative to conventional microfabrication methods. In μCP, a poly(dimethylsiloxane) (PDMS) stamp is inked with a solution of a thiol and placed on a gold substrate, facilitating thiol transfer. Regions not coated in the initial step may be functionalized with a second thiol in a solution-phase deposition step. μCP has been very widely used because it offers a rapid, inexpensive and highly effective means of patterning monolayers on sub-micrometer length scales. At the nanometer scale, dip-pen nanolithography (DPN)[5] presents a nanoscopic analogue of μCP. An atomic force microscope (AFM) tip is inked in the appropriate thiol solution, and used to trace features across a surface. DPN offers a resolution significantly better than 100 nm for alkylthiolate inks, and a variety of highly sophisticated adaptations of the technique have been reported, including parallel writing devices.[6]

An alternate route is the photopatterning of alkylthiolate SAMs by exposure to UV light through a mask (**Figure 1a**).[7] This causes photo-oxidation of the adsorbate to yield a sulfonate species, which is only weakly adsorbed and may be displaced in a simple solution-phase process. An advantage of this approach is that the first-formed SAM exhibits a very high degree of order. Illumination at ca. 250 nm is required, to initiate hot electron formation leading to SAM photo-oxidation. While many mercury lamps emit at this wavelength, their emission spectra depend quite strongly on the nature of the source. The best approach is to use a UV laser (e.g. a frequency-doubled argon ion laser). At the nanometer scale, a scanning near-field optical microscope may be coupled to a UV laser and used to carry out exposure of the SAM (**Figure 1b**).[8] For complete photo-oxidation of the SAM, an exposure of ~1-4 J cm^{-2} is required, depending on tail group and chain length. Subsequently, photo-oxidized adsorbates may be replaced in a solution-phase process. In this approach, called scanning near-field photolithography, structures as small as 9 nm may be fabricated.[9]

(a)

UV

RSO$_3^-$

RCH$_3$ RCOOH

(b) Excitation source

Mounting with electrical connections

Detector

Driving oscillation
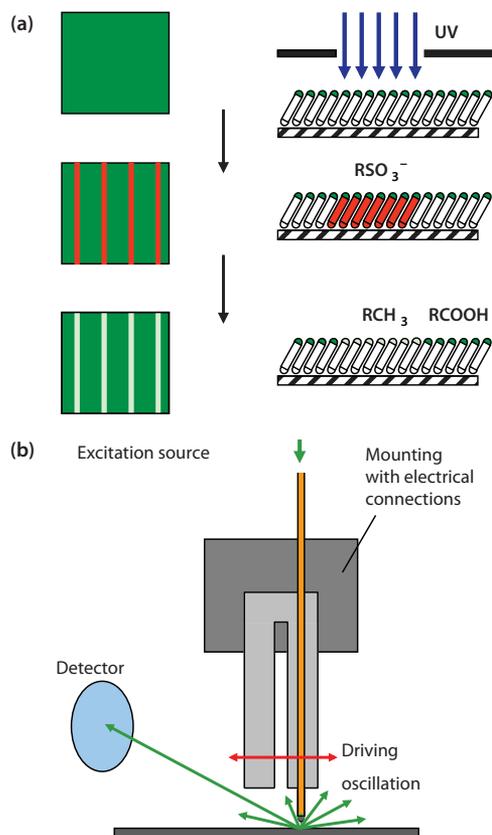
Figure 1. a) Schematic diagram showing the photopatterning of a SAM of alkylthiolates on gold. b) In scanning near-field photolithography, a near-field probe is utilized to carry out exposure with a resolution that may be as good as 9 nm (ca. λ/30).

Alkylsilane SAMs

Alkoxysilanes and trichlorosilanes react with silanol groups at silica surfaces to yield strongly bound films with exceptional oxidative and thermal stability. The biggest experimental challenge is to control polymerization between adsorbates, typically driven by the presence of too much water in the organic solvent in which the silane is typically dissolved. Polymerization can lead to the formation of rough, globular deposits. Often, silane films are thicker than a monolayer, and they typically exhibit lower degrees of ordering than alkylthiolate SAMs. In many applications, the enhanced thermal and oxidative stability and the capacity for functionalization of glass are attractive and justify the use of the more complex preparation routes. At the nanometer scale, Sagiv and co-workers have demonstrated that using an AFM with a bias voltage applied to the probe, alkylsilane SAMs may be selectively oxidized and re-functionalized with contrasting adsorbates, thus facilitating the construction of complex molecular structures.[10]

Alkylphosphonate SAMs

Oxide surfaces are important for many applications. For example, in the dye-sensitized solar cell, nanostructured Ti oxides are used to optimize the interfacial area and maximize electronic transfer from the dye to the semiconductor.[11] Alkylphosphonic acids (APA) adsorb strongly onto the oxides of aluminum, titanium and other metals to form SAMs that are closer packed and exhibit greater oxidative and thermal stability than do alkylthiolate monolayers. APA SAMs are stable during long periods of atmospheric exposure. Degradation is only a significant issue on extended exposure to aqueous conditions.

SAMs on Aluminum Oxide

The monolayer is formed by a simple solution-phase deposition process, involving immersion of the substrate in a dilute solution of APA in a suitable solvent (e.g. ethanol). The substrate, usually sputtered or evaporated Al, must be exposed to the ambient atmosphere for 20 to 40 minutes to allow the surface to become hydroxylated. During SAM formation, the APA head group is thought to be deprotonated, and interacts strongly with the oxide surface. The spacing between head groups is slightly smaller (4.8 Å) than is the case in alkylthiolate SAMs. Vibrational spectroscopy indicates that the numbers of *gauche* defects are extremely small, indicating that the adsorbates adopt a highly ordered all-*trans* conformation. Alkylphosphonate SAMs offer enormous promise for many applications, and are perhaps the most under-exploited of the SAM systems.

NH$_2$
CH$_3$
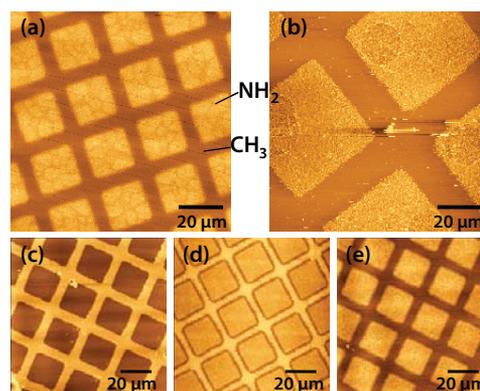
Figure 2. a) Pattern of squares of aminobutylphosphonic acid (**Sigma Prod. No. A0664**) formed in an octadecylphosphonic acid (**Aldrich Prod. No 715166**) SAM on aluminum oxide by photolithography. Following exposure of the methyl terminated SAM through a mask, the sample was immersed in a solution of the amine functionalized adsorbate to re-functionalize the degraded regions. **b)** A similar sample to the one shown in (a) following attachment of aldehyde-functionalized polymer nanoparticles. c) – e): photopatterned octadecylphosphonic acid SAMs following UV exposure and subsequent etching in sodium hydroxide. Exposures / J cm^{-2}: (a) 10, (b) 10, (c) 2, (d) 20, and (e) 40.

Compared to alkylthiolate SAMs, very little work has been done on the patterning of APA monolayers. However, photopatterning offers a simple approach.[12] On exposure to UV light with a wavelength of ca. 250 nm, the P-C bond in the adsorbate is cleaved, leading to removal of the alkyl tail. The phosphonate group is thought to remain at the surface, but this does not prevent the re-functionalization of the modified region by a second, contrasting APA. The result is a pattern of different chemical composition. **Figure 2a** shows an image of a pattern created in an APA SAM by photolithography. A mask was placed over a monolayer of octadecylphosphonic acid (ODPA, Aldrich Prod. No. 715166), and the sample was exposed to UV light. After exposure, the mask was removed and the sample immersed in an aqueous solution of aminobutylphosphonic acid (ABPA, Sigma Prod. No. A0664). The sample was imaged by friction force microscopy (FFM), a form of atomic force microscopy in which lateral deflections of the cantilever, determined by surface friction, are measured, so that the hydrophilic regions exhibit bright contrast (i.e., increased friction). **Figure 2b** shows a similar sample following attachment of aldehyde-functionalized poly-mer nanoparticles, via imine bond formation, illustrating that such approaches form a simple, effective means of building up more complex molecular structures on oxide surfaces.

Alternatively, after the UV exposure, the patterned ODPA layer may be used as a resist to etch structures into the underlying Al film. **Figure 2c** shows a sample exposed to 2 J cm^{-2} of irradiation at 244 nm. On immersion in a solution of sodium hydroxide, the exposed areas (squares) were etched, leaving the regions covered by intact adsorbates unmodified. APA SAMs behave as "switchable resists", where increasing the UV exposure gradually modifies the behavior (perhaps through

For questions, product data, or new product suggestions, please contact Aldrich Materials Science at *matsci@sial.com*.

23

ALDRICH
Materials Science

remodeling of the oxide in the exposed areas) such that at an exposure of 40 J cm^{-2} (**Figure 2e**) the patterned SAM effectively behaves as a negative tone resist, with etching being fastest in regions masked during exposure. Exposure of the APA SAM using a near-field probe enables the fabrication of nanostructures by wet chemical etching. **Figure 3** shows two images of a series of lines that have been formed by scanning near-field photolithography (SNP). The line width is ca. 100 nm. The principal limitation on resolution appears to be the rather large grain size of the Al film as better results have been obtained previously for gold films.
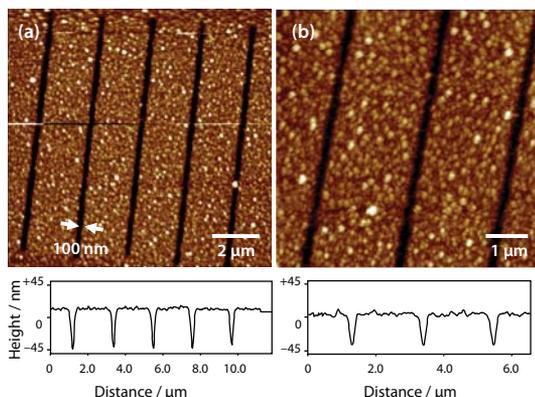
Figure 3. Tapping mode AFM images of nanostructures formed by using SNP-patterned phosphonic acid monolayers as resists for the etching of Al.

SAMs on Titanium Oxide

Titania exhibits a well-documented photocatalytic effect: absorption of UV light creates electron-hole pairs at the oxide surface leading to the oxidative breakdown of organic matter. This enables the rapid photopatterning of APA on Ti.[13] **Figure 4** shows contact angle data for a variety of SAMs on titania, and for monolayers of decyl phosphonic acid (DPA) on alumina. Following UV exposure, degradation of the alkyl chain exposes the underlying polar oxide surface and causes a decrease in the contact angle. It is clear that the rate of change is much faster on titania: even the longest adsorbate, ODPA, is degraded much faster than a SAM of DPA on alumina. Longer wavelengths are also useable for SAMs on titania than is the case on alumina; provided the photon energy is greater than the titania band gap, oxidation will occur. Shorter wavelengths are necessary on alumina because direct scission of a C-P bond is the initial step in the process.
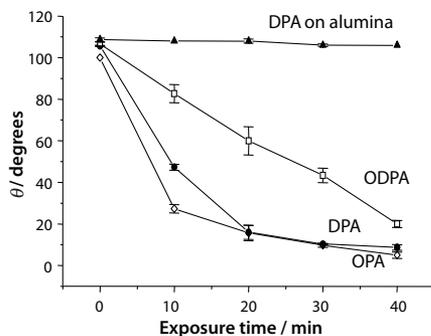
Figure 4. The variation in the contact angle with the immersion time in water for SAMs of octyl- (OPA), decyl- (DPA) and octadecyl phosphonic acids (ODPA) on the native oxide of titanium, and for DPA on alumina.

Figure 5a shows an FFM image of a SAM of ODPA following UV exposure through a mask. The exposed regions (squares) exhibit bright contrast because the underlying substrate has been exposed, yielding a localized increase in the surface free energy that causes an increase in the coefficient of friction. **Figure 5b** shows a pattern fabricated using the

same UV degradation chemistry, but with a near field probe as the light source. The functionalization of patterned SAMs on titania is demonstrated in the optical micrograph in **Figure 5c**, which shows a fluorescence emitted from aldhehyde-functionalized, dye-loaded polymer nanoparticles coupled to ABPA adsorbed into oxide regions exposed by photopatterning. Finally, **Figure 5d** shows a sample that has been patterned by exposure of an ODPA SAM followed by solution-phase etching with potassium hydroxide. Similar kind of exposure-dependent switchable character has been reported for SAMs on Ti. The nature of the behavior is also dependent on the etch solution: a sample prepared in exactly the same way to that shown in **Figure 5d** but etched with piranha solution yielded inverted contrast (i.e., the patterned SAM appeared to exhibit positive tone character, as opposed to the negative tone character shown).
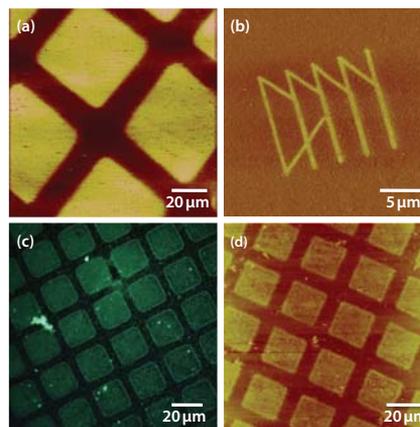
Figure 5. a) FFM image of an ODPA SAM on the native oxide of titanium following exposure through a mask (600 mesh) at 50 mW for 2 min (7.5 J cm^{-2}). Z-scale range: 0 – 517 mV. **b)** FFM image of a pattern produced in an ODPA monolayer on titanium oxide using scanning near-field photolithography. z-scale range: 0 – 1.00 V. **c)** Fluorescence microscopy image of a similar sample to that shown in (a) but where the exposed areas have been functionalized first with ABPA and then, subsequently, with aldehyde-functionalized polymer nanoparticles loaded with a fluorescent dye. **d)** A sample that has been etched in sodium hydroxide following exposure of an ODPA SAM.

Conclusions

Self-assembled monolayers of alkyl phosphonic acids are under-exploited in nanoscience. They exhibit extremely good oxidative stability, and can be readily patterned using photolithographic techniques. A wide range of functionalization strategies is accessible, via simple replacement of photodegradaed adsorbates or by wet etching of patterned monolayers. The photocatalytic degradation of SAMs on titania enables the rapid patterning of SAMs over a broad range of wavelengths.

References

(1) Netzer, L.; Sagiv, J. *J. Am. Chem. Soc.* **1983**, *105*, 674.
(2) Nuzzo, R. G.; Allara, D. L. *J. Am. Chem. Soc.* **1983**, *105*, 4481.
(3) Love, J. C.; Estroff, L. A.; Kriebel, J. K.; Nuzzo, R. G.; Whitesides, G. M. *Chem. Rev.* **2005**, *105*, 1103.
(4) Xia, Y.; Whitesides, G. M. *Angew. Chem. Int. Ed.* **1998**, *37*, 550.
(5) Piner, R. D.; Zhu, J.; Xu, F.; Hong, S.; Mirkin, C. A. *Science* **1999**, *283*, 661.
(6) Salaita, K.; Wang, Y.; Fragala, J.; Vega, R. A.; Liu, C.; Mirkin, C. A. *Angew. Chem. Int. Ed.* **2006**, *45*, 7220.
(7) Leggett, G. J. *Chem. Soc. Rev.* **2006**, *35*, 1150.
(8) Sun, S.; Chong, K. S. L.; Leggett, G. J. *J. Am Chem. Soc.* **2002**, *124*, 2414.
(9) Montague, M.; Ducker, R. E.; Chong, K. S. L.; Manning, R. J.; Rutten, F. J. M.; Davies, M. C.; Leggett, G. J. *Langmuir* **2007**, *23*, 7328.
(10) Maoz, R.; Cohen, S. R.; Sagiv, J. *Adv. Mater.* **1999**, *11*, 55.
(11) O'Regan, B.; Gratzel, M. *Nature* **1991**, *353*, 737.
(12) Sun, S.; Leggett, G. J. *Nano Lett.* **2007**, *7*, 3753.
(13) Tizazu, G.; Adawi, A.; Leggett, G. J.; Lidzey, D. G. *Langmuir* **2009**, *25*, 10746.

Self-Assembly Materials

For a complete list of available products, please visit *aldrich.com/selfassembly*

Phosphonic Acids

Name	Structure	Purity	Prod. No.
Octylphosphonic acid, n-Octylphosphonic acid, OPA	$CH_3(CH_2)_6CH_2-P(=O)(OH)-OH$	*	735914-1G 735914-5G
Tetradecylphosphonic acid, TDPA	$CH_3(CH_2)_{12}CH_2-P(=O)(OH)-OH$	*	736414-1G 736414-5G
Hexadecylphosphonic acid, HDPA	$CH_3(CH_2)_{14}CH_2-P(=O)(OH)-OH$	*	736244-1G 736244-5G
Octadecylphosphonic acid, ODPA	$CH_3(CH_2)_{16}CH_2-P(=O)(OH)-OH$	97%	715166-1G
1,8-Octanediphosphonic acid	$HO-P(=O)(OH)-CH_2(CH_2)_6CH_2-P(=O)(OH)-OH$	97%	699888-1G
1,10-Decyldiphosphonic acid	$HO-P(=O)(OH)-CH_2(CH_2)_8CH_2-P(=O)(OH)-OH$	*	737410-1G
(12-Phosphonododecyl)phosphonic acid	$HO-P(=O)(OH)-CH_2(CH_2)_{10}CH_2-P(=O)(OH)-OH$	97%	685437-1G
6-Phosphonohexanoic acid, PHA	$HO-P(=O)(OH)-\cdots-C(=O)OH$	97%	693839-1G
11-Phosphonoundecanoic acid	$HO-P(=O)(OH)-CH_2(CH_2)_8CH_2-C(=O)OH$	96%	678031-1G
16-Phosphonohexadecanoic acid	$HO-P(=O)(OH)-CH_2(CH_2)_{13}CH_2-C(=O)OH$	97%	685801-1G
4-Aminobutylphosphonic acid	$H_2NCH_2CH_2CH_2CH_2-P(=O)(OH)-OH$	≥99%	A0664-250MG A0664-1G
11-Mercaptoundecylphosphoric acid	$HSCH_2(CH_2)_9CH_2O-P(=O)(OH)-OH$	95%	674311-50MG

*For updated purities, please visit the Sigma-Aldrich website at *sigma-aldrich.com*

Thiols

Name	Structure	Purity	Prod. No.
1-Propanethiol, 1-PT	$CH_3CH_2CH_2SH$	99%	P50757-100ML P50757-500ML P50757-2L
1-Butanethiol, BT	$H_3C\diagup\diagdown SH$	99%	112925-250ML 112925-1L
1-Pentanethiol, PT	$CH_3(CH_2)_3CH_2SH$	98%	P7908-25G-A P7908-100G-A
1-Hexanethiol, HT	$CH_3(CH_2)_4CH_2SH$	95%	234192-5ML 234192-100ML 234192-500ML
1-Heptanethiol, HT	$CH_3(CH_2)_5CH_2SH$	98%	H4506-25G-A
1-Octanethiol, OT	$CH_3(CH_2)_6CH_2SH$	≥98.5%	471836-25ML 471836-100ML 471836-250ML 471836-1L 471836-2L 471836-5L
1-Nonanethiol, NT	$CH_3(CH_2)_7CH_2SH$	99%	674273-250MG
1-Decanethiol, DT	$CH_3(CH_2)_8CH_2SH$	99%	705233-1G
1-Undecanethiol, UT	$CH_3(CH_2)_9CH_2SH$	98%	510467-5G

For questions, product data, or new product suggestions, please contact Aldrich Materials Science at *matsci@sial.com*.

Name	Structure	Purity	Prod. No.
1-Dodecanethiol, DDT	$CH_3(CH_2)_{10}CH_2SH$	≥98%	471364-100ML 471364-500ML 471364-2L 471364-18L
1-Tetradecanethiol, TDT	$CH_3(CH_2)_{12}CH_2SH$	≥98.0%, GC	87193-5ML 87193-25ML
1-Pentadecanethiol, PDT	$CH_3(CH_2)_{13}CH_2SH$	98%	516295-1G
1-Hexadecanethiol, HDT	$CH_3(CH_2)_{14}CH_2SH$	99%	674516-500MG
1-Octadecanethiol, ODT	$CH_3(CH_2)_{16}CH_2SH$	98%	O1858-25ML O1858-100ML
4-Mercapto-1-butanol, MB, MCB	HS⌒⌒OH	95%	451878-1G 451878-5G
6-Mercapto-1-hexanol, MH	$SHCH_2(CH_2)_4CH_2OH$	97%	451088-5ML 451088-25ML
8-Mercapto-1-octanol, MO	$HSCH_2(CH_2)_6CH_2OH$	98%	706922-1G
11-Mercapto-1-undecanol, MUD	$HSCH_2(CH_2)_9CH_2OH$	99%	674249-250MG
11-Amino-1-undecanethiol hydro-chloride, AUT	$HSCH_2(CH_2)_9CH_2NH_2 \cdot HCl$	99%	674397-50MG
6-Mercaptohexanoic acid, MHA	HS⌒⌒⌒C(=O)OH	90%	674974-1G
8-Mercaptooctanoic acid, MOA	$HSCH_2(CH_2)_5CH_2$C(=O)OH	95%	675075-1G
11-Mercaptoundecanoic acid, MUDA	$HSCH_2(CH_2)_8CH_2$C(=O)OH	99%	674427-500MG
12-Mercaptododecanoic acid, MDA	$HSCH_2(CH_2)_9CH_2$C(=O)OH	99%	705241-250MG 705241-500MG
16-Mercaptohexadecanoic acid, MHDA	$HSCH_2(CH_2)_{13}CH_2$C(=O)OH	99%	674435-250MG
12-Mercaptododecanoic acid NHS ester	$HSCH_2(CH_2)_9CH_2$C(=O)O-NHS	97%	723061-500MG
Triethylene glycol mono-11-mercap-toundecyl ether	$HSCH_2(CH_2)_9CH_2O$⌒O⌒O⌒OH	95%	673110-250MG
(11-Mercaptoundecyl)tetra(ethylene glycol), MUTEG	$HSCH_2(CH_2)_9CH_2O$⌒O⌒O⌒O⌒OH	95%	674508-250MG
(11-Mercaptoundecyl)hexa(ethylene glycol), MUHEG	HO[⌒O]$_5$$OCH_2(CH_2)_9CH_2SH$	95%	675105-250MG
Cyclohexanethiol, CHT	⬡-SH	97%	C105600-25G C105600-100G
1-Adamantanethiol, ADT	adamantane-SH	99%, GC	719234-500MG
Thiophenol, TP	C6H5-SH	97%	T32808-100G T32808-500G T32808-1KG
2-Phenylethanethiol, PET	C6H5CH2CH2-SH	98%	252581-10G
1-Naphthalenethiol, NT	naphthalene-SH	99%	724742-5G
1,1′,4′,1″-Terphenyl-4-thiol, TPT	terphenyl-SH	97%	708488-500MG
6-(Ferrocenyl)hexanethiol, FHT	ferrocenyl⌒⌒⌒SH, Fe	–	682527-250MG
11-(1H-pyrrol-1-yl)undecane-1-thiol, PUT	pyrrole-N-$CH_2(CH_2)_9CH_2SH$	96%	717223-1G
1-(11-Mercaptoundecyl)imidazole, MUI	imidazole-N-$CH_2(CH_2)_9CH_2SH$	96%	723088-500MG

Name	Structure	Purity	Prod. No.
11-Mercaptoundecylhydroquinone, MUH		95%	728640-500MG
1,4-Benzenedimethanethiol, BDT		98%	147273-250MG 147273-1G
Biphenyl-4,4'-dithiol, BPDT		95%	673099-1G
4,4'-Bis(mercaptomethyl)biphenyl, MMB		97%	716049-1G
4,4'-Dimercaptostilbene		>96%	701696-100MG
p-Terphenyl-4,4''-dithiol, TPDT		96%	704709-1G

Polymer Materials for Stamping

For a complete list of available products, please visit *aldrich.com/stamps*

PMMA-based Resins

Name	Structure	Molecular Weight	Prod. No.
Poly(methyl methacrylate), PMMA		average M_w ~15,000 by GPC	200336-50G 200336-100G
Poly(methyl methacrylate), PMMA		average M_n 46,000 (Typical) average M_w 97,000 (Typical)	370037-25G
Poly(methyl methacrylate), PMMA		average M_w ~120,000 by GPC	182230-25G 182230-500G 182230-1KG
Poly(methyl methacrylate), PMMA		average M_w ~350,000 by GPC	445746-25G 445746-500G 445746-1KG
Poly(methyl methacrylate), PMMA		average M_w ~996,000 by GPC	182265-25G 182265-500G 182265-1KG
Poly(methyl methacrylate), isotactic, PMMA		-	452130-1G
Poly(ethyl methacrylate), PEMA		average M_n 126,000 (Typical) average M_w 340,000 (Typical)	183350-25G
Poly(ethyl methacrylate), PEMA		average M_w ~515,000 by GPC	182087-5G 182087-250G
Poly(butyl methacrylate), PBMA		average M_w ~337,000 by GPC	181528-5G 181528-250G 181528-500G
Poly(isobutyl methacrylate), PiBMA		average M_w ~70,000	181544-50G 181544-250G
Poly(isobutyl methacrylate), PiBMA		average M_w ~130,000	445754-50G
Poly(isobutyl methacrylate), PiBMA		average M_n 140,000 (Typical) average M_w 300,000 (Typical)	181552-5G 181552-25G
Poly(hexyl methacrylate) solution, PHMA		average M_w ~400,000 by GPC	182125-25G
Poly(2-ethylhexyl methacrylate) solution, PEHMA		average M_w ~123,000 by GPC	182079-50G
Poly(lauryl methacrylate) solution, PLMA		average M_n 150,000 (Typical) average M_w 470,000 (Typical)	182192-5G

For questions, product data, or new product suggestions, please contact Aldrich Materials Science at *matsci@sial.com*.

ALDRICH® Materials Science

27

Name	Structure	Molecular Weight	Prod. No.
Poly(2-hydroxyethyl methacrylate), PHEMA		average M_v ~20,000	529265-5G 529265-25G
Poly(2-hydroxyethyl methacrylate), PHEMA		average M_v ~300,000	192066-10G 192066-25G
Poly(2-hydroxyethyl methacrylate), PHEMA		average M_v ~1,000,000	529257-1G 529257-10G
Poly(2-hydroxypropyl methacrylate), PHPMA		-	182133-10G
Poly(cyclohexyl methacrylate), PCMA		average M_w ~65,000 by GPC	191949-25G
Poly(benzyl methacrylate), PBMA		average M_w ~70,000 by GPC	181358-10G
Poly(methyl methacrylate-co-ethyl acrylate), PMMA-co-EA		average M_n ~39,500 by GPC average M_w ~101,000 by GPC	182249-25G 182249-500G 182249-1KG
Poly(methyl methacrylate-co-methacrylic acid), PMMA-co-MA		average M_n ~15,000 by GPC average M_w ~34,000 by GPC	376914-25G 376914-500G 376914-1KG
Poly(butyl methacrylate-co-methyl methacrylate), PBMA-co-MMA		average M_w ~150,000	474037-250G
Poly(methyl methacrylate-co-ethylene glycol dimethacrylate)		-	463183-500G
Poly(methyl methacrylate-co-ethylene glycol dimethacrylate)		-	463167-500G
Poly(styrene-co-methyl methacrylate), PS-co-MMA		average M_w 100,000-150,000	462896-250G
Poly(4-vinylphenol-co-methyl methacrylate), PVP-co-PMMA		-	474576-50G
Poly(4-vinylpyridine-co-butyl methacrylate)		-	306258-50G
Poly(ethylene-co-glycidyl methacrylate)		-	430862-250G
Poly(1-vinylpyrrolidone-co-2-dimethylaminoethyl methacrylate) solution		average M_w ~1,000,000 by GPC	434469-250ML 434469-1L
Poly[(2-ethyldimethylammonioethyl methacrylate ethyl sulfate)-co-(1-vinylpyrrolidone)]		average M_w <1,000,000 by GPC	190888-250G

PDMS-based Resins

Name	Structure	Molecular Weight	Prod. No.
Kit for Creating Hydrophilic PDMS Surface		-	701912-1KT
Polycarbomethylsilane, PCMS		average M_w ~800	522589-25G
Poly(dimethylsiloxane), hydroxy terminated, PDMS		-	481955-100ML 481955-500ML
Poly(dimethylsiloxane), hydroxy terminated, PDMS		-	481963-100ML 481963-500ML
Poly(dimethylsiloxane), hydride terminated, PDMS		average M_n ~580	423785-50ML 423785-250ML
Poly(methylhydrosiloxane), trimethylsilyl terminated, PDMS		average M_n ~390	482382-20ML
Poly(methylhydrosiloxane), PMHS		average M_n 1,700-3,200	176206-50G 176206-250G
Poly(dimethylsiloxane-co-methylhydrosiloxane), trimethylsilyl terminated		average M_n ~950	482196-50ML
Poly(dimethylsiloxane-co-methylhydrosiloxane), trimethylsilyl terminated		average M_n ~13,000	482374-25ML 482374-150ML
Poly(dimethylsiloxane), vinyl terminated, PDMS		average M_w ~25,000	433012-100ML 433012-500ML
Poly(dimethylsiloxane), bis(hydroxyalkyl) terminated, PDMS		average M_n ~5,600	481246-25ML 481246-100ML
Poly(dimethylsiloxane), bis(3-aminopropyl) terminated, PDMS		average M_n ~2,500	481688-10ML 481688-50ML
Poly(dimethylsiloxane), bis(3-aminopropyl) terminated, PDMS		average M_n ~27,000	481696-50ML
Poly(dimethylsiloxane), diglycidyl ether terminated, PDMS		M_n ~800	480282-50ML 480282-250ML
Poly(dimethylsiloxane), monoglycidyl ether terminated, PDMS		average M_n ~5,000	480290-25ML
Poly(dimethylsiloxane), monohydroxy terminated, PDMS		average M_n ~4,670	480355-50ML
Poly[dimethylsiloxane-co-(3-aminopropyl) methylsiloxane], PDMS		-	480304-50ML 480304-250ML
Poly[dimethylsiloxane-co-[3-(2-(2-hydroxyethoxy) ethoxy)propyl]methylsiloxane], PDMS		-	480320-250ML
Poly[dimethylsiloxane-co-methyl(3-hydroxypropyl) siloxane]-graft-poly(ethylene glycol) methyl ether, PDMS		-	482412-50ML

For questions, product data, or new product suggestions, please contact Aldrich Materials Science at *matsci@sial.com*.

29

Sigma-Aldrich® Worldwide Offices

Argentina
Free Tel: 0810 888 7446
Tel: (+54) 11 4556 1472
Fax: (+54) 11 4552 1698

Australia
Free Tel: 1800 800 097
Free Fax: 1800 800 096
Tel: (+61) 2 9841 0555
Fax: (+61) 2 9841 0500

Austria
Tel: (+43) 1 605 81 10
Fax: (+43) 1 605 81 20

Belgium
Free Tel: 0800 14747
Free Fax: 0800 14745
Tel: (+32) 3 899 13 01
Fax: (+32) 3 899 13 11

Brazil
Free Tel: 0800 701 7425
Tel: (+55) 11 3732 3100
Fax: (+55) 11 5522 9895

Canada
Free Tel: 1800 565 1400
Free Fax: 1800 265 3858
Tel: (+1) 905 829 9500
Fax: (+1) 905 829 9292

Chile
Tel: (+56) 2 495 7395
Fax: (+56) 2 495 7396

China
Free Tel: 800 819 3336
Tel: (+86) 21 6141 5566
Fax: (+86) 21 6141 5567

Czech Republic
Tel: (+420) 246 003 200
Fax: (+420) 246 003 291

Denmark
Tel: (+45) 43 56 59 00
Fax: (+45) 43 56 59 05

Finland
Tel: (+358) 9 350 9250
Fax: (+358) 9 350 92555

France
Free Tel: 0800 211 408
Free Fax: 0800 031 052
Tel: (+33) 474 82 28 88
Fax: (+33) 474 95 68 08

Germany
Free Tel: 0800 51 55 000
Free Fax: 0800 64 90 000
Tel: (+49) 89 6513 0
Fax: (+49) 89 6513 1160

Hungary
Ingyenes telefonszám: 06 80 355 355
Ingyenes fax szám: 06 80 344 344
Tel: (+36) 1 235 9063
Fax: (+36) 1 269 6470

India
Telephone
Bangalore: (+91) 80 6621 9400
New Delhi: (+91) 11 4358 8000
Mumbai: (+91) 22 4087 2364
Hyderabad: (+91) 40 4015 5488
Kolkata: (+91) 33 4013 8000

Fax
Bangalore: (+91) 80 6621 9550
New Delhi: (+91) 11 4358 8001
Mumbai: (+91) 22 2579 7589
Hyderabad: (+91) 40 4015 5466
Kolkata: (+91) 33 4013 8016

Ireland
Free Tel: 1800 200 888
Free Fax: 1800 600 222
Tel: (+353) 402 20370
Fax: (+ 353) 402 20375

Israel
Free Tel: 1 800 70 2222
Tel: (+972) 8 948 4100
Fax: (+972) 8 948 4200

Italy
Free Tel: 800 827 018
Tel: (+39) 02 3341 7310
Fax: (+39) 02 3801 0737

Japan
Tel: (+81) 3 5796 7300
Fax: (+81) 3 5796 7315

Korea
Free Tel: (+82) 80 023 7111
Free Fax: (+82) 80 023 8111
Tel: (+82) 31 329 9000
Fax: (+82) 31 329 9090

Malaysia
Tel: (+60) 3 5635 3321
Fax: (+60) 3 5635 4116

Mexico
Free Tel: 01 800 007 5300
Free Fax: 01 800 712 9920
Tel: (+52) 722 276 1600
Fax: (+52) 722 276 1601

The Netherlands
Free Tel: 0800 022 9088
Free Fax: 0800 022 9089
Tel: (+31) 78 620 5411
Fax: (+31) 78 620 5421

New Zealand
Free Tel: 0800 936 666
Free Fax: 0800 937 777
Tel: (+61) 2 9841 0555
Fax: (+61) 2 9841 0500

Norway
Tel: (+47) 23 17 60 00
Fax: (+47) 23 17 60 10

Poland
Tel: (+48) 61 829 01 00
Fax: (+48) 61 829 01 20

Portugal
Free Tel: 800 202 180
Free Fax: 800 202 178
Tel: (+351) 21 924 2555
Fax: (+351) 21 924 2610

Russia
Tel: (+7) 495 621 5828
Fax: (+7) 495 621 6037

Singapore
Tel: (+65) 6779 1200
Fax: (+65) 6779 1822

Slovakia
Tel: (+421) 255 571 562
Fax: (+421) 255 571 564

South Africa
Free Tel: 0800 1100 75
Free Fax: 0800 1100 79
Tel: (+27) 11 979 1188
Fax: (+27) 11 979 1119

Spain
Free Tel: 900 101 376
Free Fax: 900 102 028
Tel: (+34) 91 661 99 77
Fax: (+34) 91 661 96 42

Sweden
Tel: (+46) 8 742 4200
Fax: (+46) 8 742 4243

Switzerland
Free Tel: 0800 80 00 80
Free Fax: 0800 80 00 81
Tel: (+41) 81 755 2828
Fax: (+41) 81 755 2815

United Kingdom
Free Tel: 0800 717 181
Free Fax: 0800 378 785
Tel: (+44) 1747 833 000
Fax: (+44) 1747 833 313

United States
Toll-Free: 800 325 3010
Toll-Free Fax: 800 325 5052
Tel: (+1) 314 771 5765
Fax: (+1) 314 771 5757

Vietnam
Tel: (+84) 3516 2810
Fax: (+84) 6258 4238

Internet
sigma-aldrich.com

Enabling Science to
Improve the Quality of Life

Order/Customer Service (800) 325-3010 • Fax (800) 325-5052
Technical Service (800) 325-5832 • *sigma-aldrich.com/techservice*
Development/Custom Manufacturing Inquiries SAFC® (800) 244-1173
Safety-related Information *sigma-aldrich.com/safetycenter*

World Headquarters
3050 Spruce St.
St. Louis, MO 63103
(314) 771-5765
sigma-aldrich.com

SIGMA-ALDRICH®